N72-23664
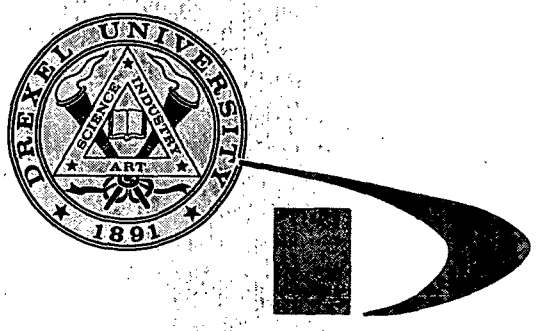
CASE FILE COPY

DEVELOPMENT OF VISUAL-DISPLAY

AID TO AIR NAVIGATION

Annual Report

NASA Grant NGR 39-004-038

1 January 1971 to 31 December 1971

drexel university

DEVELOPMENT OF VISUAL-DISPLAY

AID TO AIR NAVIGATION

Annual Report

NASA Grant NGR 39-004-038

1 January 1971 to 31 December 1971

Submitted by

Professor T. J. Matcovich

Drexel University

Philadelphia, Pennsylvania 19104

TABLE OF CONTENTS

LIST OF FIGURES

SECTION 1

INTRODUCTION

1.1 Objective

The objective of the work described in this report is to design, develop and fabricate a "visual-display" aid to air navigation. The display will locate an aircraft on a standard navigational chart when activated by two independent directional signals. A prime consideration is to make the display sufficiently inexpensive to encourage its wide spread use in private as well as commercial aircraft.

1.2 Display Concept

The display, shown in Figure 1.1, will comprise a radial pattern of electrically conductive line pairs, liquid crystal material contained between the line pairs, and addressing and activating electronics. The display will be placed over a standard aircraft map and centered on an appropriate VOR station. The VOR signals will be processed to produce the address of the radial line pair most closely corresponding to the VOR station direction. A voltage will be applied to the addressed line pair and the liquid crystal will respond by becoming milky-white. Since the liquid crystal between the other line pairs will remain transparent the VOR station direction will be clearly indicated by the selected line pair. Positional data will be obtained by placing two radial patterns on the map and observing the intersection of the two selected pairs of radial lines.

1.3 Scope of Program

The scope of the program described in this report included the design and fabrication of a liquid crystal display, but did not include the design of the electronics. Demonstration models were fabricated from available liquid crystal materials; however, no attempt was made to synthesize liquid crystals. The program also included a study of the stability of liquid crystal cells.

A continuation of this grant has been provided to develop the required electronics and fabricate an operational display.

1.4 Program Organization

The work described in this report was performed at Drexel University in the graduate research laboratories of the Physics and Electrical Engineering Departments including: Professor Lord's laboratory in Disque Hall; Professor Herczfeld's semiconductor laboratory in Stratton Hall; and Professor Matcovich's microelectronics laboratory in Stratton Hall. Three faculty members and four students were engaged in this work. The names of the participants and the fraction of their time assigned to the program are given in Appendix A.

1.5 Summary of Results

Sample quantities of four commercially available, room-temperature nematic liquid crystals were purchased. The contrast ratio obtainable with all these materials were comparable, but two had significantly longer lifetimes. Some samples still on test have operated continuously for over 15 weeks.

The liquid crystals were life tested in cells made from different electrode materials; gold, copper, aluminum, tin oxide and indium oxide electrodes were used. Higher contrast ratios were consistently measured for cells made with gold electrodes. This is apparently due to a tendency of the liquid crystal molecules to align perpendicular to the gold surface. The failure rate for cells made from copper electrodes was much higher than that for cells made from other electrode materials.

Cells operated on dc voltage failed in very short periods of time; the use of ac excitation voltages is essential to long cell life.

The visibility of liquid crystal filled lines was studied. Lines should be 20 to 30 mils wide for good visibility. Pulsed operation at a few cycles-per-second significantly improved visibility. Use of a reflective backing also improved visibility.

Several line geometries were studied. These included parallel configurations (light direction parallel to E field) and perpendicular configurations (light direction perpendicular to E field). An edge configuration which was designed for ease of fabrication was also evaluated. The parallel configuration worked well but had fabrication and material problems. The perpendicular configuration had lower contrast and required higher operating voltage, but was easier to fabricate. The edge configuration had such poor visibility that its development was discontinued.

Experiments were performed to determine the optimum cell dimension for the parallel and perpendicular configurations. Optical path lengths of 1/4 to 1/2 mil appear optimum. Electric field requirements are ~60 volts/mil.

Display models were designed in both the parallel and perpendicular configurations. A full-scale, non-operative perpendicular display model will be delivered to NASA. An operative, 4-inch-long line from this display will also be delivered and demonstrated. This model will include a cover sealed in place.

In supporting work, the staff arranged two seminars on liquid crystals at Drexel and attended three conferences. The details of these activities are given in Appendix B. A literature search was also made and a Bibliography is contained in this report.

SECTION 2

BASIC DISPLAY CONFIGURATION

.The two basic configurations for the liquid crystal cells are described in Sections 2.1 and 2.2. In both cases the liquid crystal is contained between conductive electrodes and the electric field, E, due to the applied voltage is perpendicular to the electrodes. An alternate configuration which was evaluated is described in Section 2.3.

2.1 Parallel Configuration

In the parallel configuration shown in Figure 2.1a the direction of the incident light is essentially parallel to the electric field. At least one of the conductive electrodes used in this configuration must be transparent. If the dynamic scattering phenomenon is to be observed by reflected light, the back electrode should be highly reflective. If the phenomenon is to be observed by transmitted light both electrodes must be transparent. The optical path length, d, is related to the electric field, E, through the relationship: $E = V/d$ where V is the applied voltage.

2.2 Perpendicular Configuration

In the perpendicular configuration shown in Figure 2.1b the direction of the incident light is essentially perpendicular to the electric field. In this configuration transparent electrodes are not required and the optical path length is independent of the electrode spacing. A highly reflecting surface must be placed in the light beam if scattering is to be observed by reflected light.

In both configurations the resistivity of the liquid crystal cell is very high ($\sim 10^9$ ohm-cm) and only small currents flow when the voltage is applied. Although small, this current is essential to the operation of the cell and the physical design must reflect this requirement.

2.3 Edge Configuration

An alternative configuration is shown in Figure 2.2. The geometry was chosen because it was potentially easy to fabricate. The two upper electrodes are held at the same potential and the lower electrode at a different potential. The electric field is strongest along the edge and predominantly parallel to the direction of the incident light. Scattering occurs primarily in the vincinity of the edges. Experimental data indicate that the extent of the scattering area is so small that the visibility of the line is poor. Consequently, efforts to develop this configuration have been terminated.

SECTION 3

MATERIALS

3.1 Liquid Crystals

Nematic type liquid crystals were used in this study. These materials, which are normally transparent, become milky-white when a field is applied due to the "dynamic scattering" of the incident light. Several companies supply liquid crystals on a commercial basis. Most of the available nematics are in the liquid crystal state a temperatures above the normal ambient; however, four were available which did function at normal room temperature. Several others became available toward the end of this study period and will be evaluated in the continuation program (see Section 5). The available room temperature nematic liquid crystal materials are listed together with the suppliers in Appendix C.

Criteria for liquid crystal quality are contrast, operating voltage, stability and cost. The more recently evaluated samples appear to be more stable (Section 5) and the newer materials have a wider operating temperature range. Materials with operating voltages below 20 volts have been reported[1] in the literature but are not commercially available. The contrast ratio does not vary significantly between materials (Section 6) but

[1]"Performance Characteristics of Nematic Liquid Crystal Display Devices," L.T. Creagh, A.R. Kinetz and R.A. Reynolds, IEEE Trans. on Electron Devices, Vol. ED-18, No. 9, pp. 672-678, (September 1971).

"Deformation of Nematic Liquid Crystals with Vertical Orientation in Electric Fields," M.F. Schiekel and K. Fahrenschon, Appl. Phys. Letters, Vol. 19, pp. 391-393 (1971).

"Effects of Additions of Cholesterics on Nematic Liquid Crystal Properties," B. Kerllenevich and A. Coche, J. Appl. Phys., Vol. 42, pp. 5313-5315 (1971).

can be substantially affected by other aspects of cell construction. Although expensive when purchased in small quantities, liquid crystals are basically inexpensive.

3.2 Substrates, Covers and Conductors

Plastic substrates are used in all display models and some test samples; glass substrates are used in the other test samples. Transparent conductive substrates are available from several companies. Corning supplies tin oxide coated "Nesa" glass, PPG supplies indium oxide coated "Nesaton" glass and Liberty Glass supplies gold coated glass and plastic. The plastic is transparent and felxible. Since the liquid crystal cell resistance is high, the electrode resistivity need not be low; all the materials noted have adequate conductivity. The transparent conductors must be etched in some applications. The tin oxide coating which is fired on is very stable and difficult to etch; the indium oxide coating which is sputtered on is less stable and easily etched in HCl. The gold coating is made very thin to retain transparency and is easily etched.

Transparent, flexible substrates with thick (opaque) layers of metals are used in the display models and are available from a large number of suppliers. The criteria for the quality of a conductor clad substrate include transparency of the base, adhesion of the metal, compatibility with liquid crystals, etchability of both base and metal, dimensional stability, availability and cost. The base material is either Kapton, Mylar or polyester and ranges in thickness from one-tenth to several mils. Kapton and Mylar can be etched to form channels and this property is used

in several of the display designs. The conductor material is typically copper or aluminum and may be from 1000 Å to several mils in thickness. Adhesives are frequently used to attach the thicker conductor layers to the plastic. These can be used only if the liquid crystal does not contact the adhesive since the subsequent interaction adversely affects the crystal properties. Thick copper layers can also be obtained by electroplating thin layers; however, the usable thickness is limited since thick electroplated layers are usually under high stress. When narrow copper lines are etched the stresses cause "puckering" of the flexible base material. Most metals can be easily etched to form narrow conductor patterns; however, metal adhesion becomes very important when long narrow lines are formed on large flexible substrates. Peeling is a common problem. Materials with adequate adhesion are available, but many commercial products fail under these conditions. This will be a problem in quality control since nominally identical samples from the same manufacturer will show great variation in adhesive properties.

3.3 Processing Materials

A variety of commercial processing materials have been used in this study. These include; photoresists, developers and strippers: etchant baths for copper, aluminum, chromium and gold: plating baths for copper nickle and chromium: filters for the photoresist: cleaning detergents: and masks. These materials are in common use in the hybrid and integrated circuit industries and are available from a large number of suppliers. A partial listing of suppliers is given in Appnedix D.

SECTION 4

OPTIMIZATION OF PARAMETERS

The critical operating parameters are visibility and operating voltage. Both depend on the cell geometry and mode of operation.

4.1 Voltage and Spacing

The optimum voltage and electrode spacing to be used in parallel and perpendicular configuration cells was determined by measuring the physical contrast ratio as a function of voltage for cells of different geometries. The physical contrast ratio was measured with the equipment shown in Figure 4.1 and is defined as:

$$C.R. = \frac{I_o}{I_v} \quad \text{for transmitted light}$$

and

$$C.R. = \frac{I_v}{I_o} \quad \text{for reflected light}$$

where I_o is the transmitted (reflected) light intensity with $V = 0$

I_v is the transmitted (reflected) light intensity with $V \neq 0$

and V is the potential applied to the liquid crystal cell.

4.1.1 Parallel Configuration

Liquid crystal cells of the parallel type were studied to optimize the cell parameters. The transparent cell electrodes were made

from Nesatron glass and the liquid crystal was Eastman's MBBA No. 11246.
Mylar spacers were used to set the interelectrode spacings of 6.3, 12.7
and 30μ.

The transmitted-light physical contrast ratio was measured with
the apparatus shown in Figure 4.1a. The transmitted light contrast
ratio was measured as a function of voltage with and without the polarizer
and analyzer. Sinusoidal excitations at frequencies of 60, 200, 600, 800
and 1000 Hz were applied in addition to dc. These data are shown in
Figures 4.2 through 4.4. Best results are obtained for applied fre-
quencies between 0 and 400 Hz. The contrast ratio increases nearly
linearly with applied voltage but shows some tendency to saturate at
higher voltages. The near linear dependency precludes the coincident
voltage selection of cells in arrays. In Figure 4.5 the contrast ratio
is shown as a function of thickness for a fixed applied voltage of 80 volts.
Maximum scattering occurs at a thickness of about 12μ (1/2 mil). The con-
trast ratio does not decrease substantially when the frequency of the
applied voltage is raised to 400 Hz.

A simple model can be proposed to explain the existence of the
observed scattering maximum. For small thicknesses the electric field
is large and the number of scattering centers per unit length is large;
however, the path length through the material is short. As the thickness
is increased the path length increases but the density of scattering
centers decreases due to the decreased field strength. For thickness
less than 12μ, the effect of increased path length dominates and scattering
increases with thickness. For thickness over 12μ the decrease in density
more than compensates for the increased path length and the scattering
decreases.

The transmitted light contrast ratio obtained with polarized light is nearly twice that obtained with unpolarized light. These data were taken with the optical axis of the analyzer parallel to that of the polarizer. The results suggest that the scattering causes nearly complete depolarization of the incident light. For this condition the analyzer will reduce the intensity of the scattered incident beam by a factor of two but will not affect the intensity of the unscattered beam.

The reflected light contrast ratio was also measured as a function of voltage. The apparatus used is shown in Figure 4.1b; a laser beam light source was used and the beam made an angle of 30° with the normal. The data are shown in Figure 4.6 and 4.7. The applied voltage was dc or 60 Hz only. Polarized light was not used. The contrast ratios are substantially higher than in the transmitted light case and appear to saturate. The absolute value of contrast ratio is a strong function of the measuring technique and ratio definition. A direct comparison with the transmitted light data is not appropriate The contrast ratio is plotted as a function of thickness in Figure 4.8. Presumably the ratio peaks at 6.3 or less micron thickness; spacing narrower than 6.3μ are difficult to attain.

4.1.2 Perpendicular Configuration

Liquid crystal cells of the perpendicular type were studied to optimize the cell parameters. A typical cell is shown in Figure 4.9. The cell comprises chrome-copper electrodes on a glass substrate. The chromium was used to insure good adhesion and was evaporated. A layer of copper was also evaporated to about 5000 Å thickness and copper layers

of thickness 1/16, 1/8, 1/4, 1/2 and 1 mil were prepared by electroplating.
A channel was then etched in the conductor to achieve the geometry shown
in Figure 4.9. Channel widths of 10, 15, 17.5 and 20 mils were prepared.
The channels were carefully filled with Eastman's MBBA No. 11246 liquid
crystal by use of a microsyringe (Section 9) to prevent overflow and con-
sequent uncertainty in the optical path length. Figure 4.10 shows a typical
set of contrast vs voltage data. The data indicate that the contrast ratio
increases as the frequency of the applied voltage decreases and as the ampli-
tuden increases. Figure 4.11 shows the variation of contrast ratio with
optical path length for a spacing on 10 mils. The curve peaks at 1/2 mil
but is rather flat. Figure 4.12 shows the variation of contrast ratio with
electric field, E. The contrast ratio appears to be approaching saturation
at 60 volts/mil.

The measurements indicate that for both configurations:

the optimal optical path length is 1/2 mil (1/4 mil for reflection)
the optimal operating frequency is dc to 60 cps
the field required for saturation is 40 to 60 volts/mil.

The contrast ratio measured in the parallel configuration is
significantly higher than in the perpendicular configuration.

4.2 Visibility

Line visibility depends on many subjective quantities as well as the
physical contrast ratio. Since the "physiological" contrast, the response
of the human observer, is difficult to define and hence hard to measure a
group of observers was assembled to achieve a rough measure of this
parameter.

4.2.1 Multiple Line Geometry

The experiments with perpendicular configuration samples indicated that lines only a few mils wide were not easily visible. Consequently the multiple line pattern shown in Figure 4.13 was fabricated and tested. This display comprises five four-mil-wide lines defining four four-mil-wide spaces. This line was easily seen when activated.

4.2.2 Reflective Backing

The apparatus shown in Figure 4.14 was used to measure the intensity of the light scattered off axis. The results are shown in Figure 4.15. These data were taken on a parallel configuration cell. The liquid crystal was Eastman's MBBA No. 11246 and the spacing was 12.7μ. The data show that most of the scattered light is confined to a 20° cone about the incident light direction. Liquid crystals are forward scatterers; that is, most of the light is scattered through angles of less than 90°.

A line containing liquid crystal in a turbulent state can be distinguished from unactivated lines because it obscures the information behind it or because it reflects light more effectively. In the former case the conductive lines may be transparent and the visibility will depend on the information content of the map under the selected line. In the latter case a reflective backing need be used (since the liquid crystal is a forward scatterer) and this backing will obscure part of the map even when the line isn't selected.

An experiment was performed to determine how wide an opaque line could be placed over a typical navigation map without destroying

legibility. A set of lines 4, 10, 20 and 40 mils wide were placed over a map as shown in Figure 4.16. Opaque lines less than 40 mils wide appear to be satisfactory. The reflective line has greater visibility than the opaque line and a line 30 mils wide provides satisfactory visibility. Consequently, designs have been based on the use of reflective lines.

4.2.3 Pulsed Operation

Physiological contrast is improved if a light source flashes rather than remain constant. This contrast is a function of the flicker frequency and is usually a maximum just below the fusion frequency at which the flashing light appears to be continuous. The following test was performed to verify the applicability of this theory to the display.

A liquid crystal cell was placed over a map and operated from a pulsed voltage source. The pulse frequency was varied from 0 to 20 pulses-per-second. Several observers (Section 4.2) were asked to view the map and indicate the flashing frequency which made the cell most visible. The results, which are given in Figure 4.17 depend on whether the observer knew the location of the flashing cell. The optimum repetition rate when the observer knew the cell location was 2.5 Hz and when he did not know the location was 7.5 Hz. In all cases the visibility of the flashing display was greater than the constant display.

SECTION 5

STABILITY

5.1 Objectives and Results

Tests were conducted to determine the lifetime of a liquid crystal cell and to determine the electrode material most compatible with liquid crystals. A number of cells were constructed from the materials proposed for use in the displays. These cells were subjected to continuous electrical and mechanical stresses and their physical contrast ratio and electrical resistance were measured. The test results clearly indicate that ac voltages should be used and that bending vibration at normal cabin ambients do not affect cell operation.

5.2 Electrical Stresses

Test cells were made in the parallel configuration. The electrode spacing was 50.8μ; the electrode materials were Nesa glass; Nesatron glass, and thin layers of copper, aluminum and gold. The thin layers were made by evaporation and were transparent. Data are reported for Eastman's MBBA No. 11246, Liquid Crystal Industries room temperature liquid crystal, Merck's Licristal IV and Vari-Light's VL462N. Two new materials have been obtained, but too recently to report any data. These are a 5 to 105°C nematic from Eastman and Merck's Licristal V.

Several cells of each type were subjected to 60 Hz, 40 volt excitation and their physical contrast ratios were periodically measured. The data are shown in Table 5.1. The earliest tests are on MBBA and Liquid Crystal Industries material since the other crystals did not become available until August.

TABLE 5.1

PARALLEL CELL STABILITY DATA

Material	Electrode	Running Dates	Total Days	C.R.	Remarks
Eastman MBBA No.11246	Al	3/19 - 5/4	46	1.98	Electrode failed
		6/28 - 8/4	39	1.60	
		8/6 - 9/8	33	1.52	
		9/27 -	(81)	2.81	
		11/17 -	(30)	3.43	Electrode failed
	Au	8/6 - 8/31	25	2.42	Electrode failed
		9/27 - 11/5	39	4.40	
		11/17	(30)	4.08	
	Cu	3/25 - 6/4	71	2.22	
		6/28 - 9/13	77	1.99	Electrode failed
		9/27 - 10/15	18	2.71	Electrode failed
		11/17 - 12/17	81	2.73	
	Nesa	3/19 - 5/5	47	1.66	
		6/28 - 7/20	22	1.45	
		8/6 - 8/17	11	1.64	
		9/27	(81)	2.14	
		11/17	(30)	2.40	
	Nesatron	4/28 - 6/4	37	2.06	
		6/28 - 7/30	32	1.7	
		8/6	11	1.82	
		9/27 -	(81)	1.95	
		11/17 -	(30)	2.12	
Liquid Crystal Ind.	Al	6/28 - 7/20	22	2.09	Electrode failed
		8/6 - 99/27	52	1.96	
		9/27 - 11/5	39	2.30	
		11/17 -	(30)	3.26	
	Au	8/6 - 10/4	59	2.21	
		9/27 -	(81)	3.35	
		11/17 -	(30)	2.47	Electrode failed leaked
	Cu	6/28 - 9/27	91	2.90	
		9/27 - 11/5	39	2.14	
		11/17 -	(30)	2.46	
	Nesa	6/28 - 7/1	3	1.99	
		7/6 - 7/20	14	1.65	
		8/6 - 8/17	11	2.61	
		9/27 - 11/5	29	1.90	
		11/17 -	(30)	2.28	
	Nesatron	6/28 - 8/17	50	2.07	
		9/27 - 11/5	39	2.01	
		11/17 -	(30)	2.26	

Material	Electrode	Running Dates		Total Days	C.R.	Remarks
Merck	Al	8/4 –		(145)	2.65	
Licristal		9/27 –		(81)	2.41	
IV	Au	8/4 –	10/8	93	2.78	
		9/27 –	11/5	39	3.30	Electrode failed
	Cu	8/6 –	11/5	91	2.04	Electrode failed
		9/27 –	10/8	11	2.88	Electrode failed
	Nesa	8/4 –		(145)	1.99	
		9/27		(81)	2.16	
	Nesatron	8/4 –		(145)	2.23	
		9/27 –		(81)	1.95	
Vari-	Al	8/4 –		(145)	2.27	
Light		9/27 –		(81)	2.32	
	Au	8/4 –	8/17	13	2.77	Electrode failed
		9/27 –		(81)	4.05	
	Cu	8/6 –	9/8	33	2.23	Electrode failed
	Nesa	8/4 –		(145)	1.95	
		9/27 –		(81)	2.41	
	Nesatron	8/4 –		(145)	2.05	
		9/27 –		(81)	1.78	

( ) indicates sample is still operating

The lifetime of the Merck and Vari-Light materials is longer than the Eastman and Liquid Crystal Industries. Seven Vari-Light cells are still functioning after an average of over 15 weeks of continuous operation. Two other cells failed after 13 and 33 days due to defective electrodes.

The contrast ratio obtained from each of the liquid crystals is about the same (Section 6); however, the contrast ratio obtained with gold electrodes is significantly higher than that obtained with other electrode materials (Table 5.2). The reason for this is the liquid crystal molecules assume a preferred orientation with respect to the gold electrode. The molecules line up with their optic axes perpendicular to the substrate, whereas there is no preferred orientation with any of the other electrode materials.

A strong interaction was noted between the liquid crystal and the copper electrodes. Over 70% of the life test samples made with copper electrodes failed; the corresponding number for gold is 50% and for aluminum is 22%. Similar results with copper have been noted in the literature[2]. These data became available too late to influence the design of the display models.

[2]"Dielectric and Resistivity Measurements on Room Temperature Nematic MBBA," F. Rondelez, D. Diquet and G. Durand, Mol. Cryst. and Liq. Cryst., Vol., 15, pp. 183-188 (1971).

TABLE 5.2

AFFECT OF ELECTRODE MATERIAL ON CONTRAST RATIO

Electrode Material	Contrast Ratio
Al	2.34
Au	3.18
Cu	2.43
Nesa	2.34
Nesatron	1.99

Metallic electrode cells operated at 40 volts dc failed in short periods of time and showed definite evidence of electrode corrosion. Cells made with semitransparent electrodes of aluminum, copper and silver failed within two days when operated at 40 volts dc. In each case the anode material was completely stripped from the substrate. Cells made from Nesa and Nesatron glass were also operated at 40 volts dc; these cells failed after three days. The liquid crystal in these cells changed from light yellow to brown as the cell aged. The resistance of the anode of the Nesa glass cell was unchanged, but the cathode resistance increased by a factor of 2 and the cathode was covered with a brown stain. The resistance of the anode of the Nesatron glass cell increased by a factor of 100; the cathode resistance increased by a factor of 10 and the cathode was covered with a brown stain. The observed stripping of the anodes is due to electrolytic action. The Nesa glass would be expected to be most resistant to the deplating effect, the Nesatron glass less resistant and the metals least resistant.

In the cells that failed the discolored liquid crystals appeared to be isotropic. These data suggest that the transition temperature from isotropic liquid to liquid crystal was lowered. To test this theory a special cell was made and the transition temperature was measured as a function of operating time. The interelectrode spacing of this cell was 19μ, the electrode material was Nesa glass and the liquid crystal was MBBA. The cell was operated at 20 dc volts with the results shown in Figure 5.1. The transition temperature decreased in a linear fashion at a rate of 3.4°C per day. Two additional tests on similar MBBA cells showed 8 and 27°C per day rates-of-change in the transition temperature.

5.3 Mechanical Stress

Ultrasonic vibration is known to affect the operation of liquid crystals. Since the display device will be subjected to vibration in its normal environments, tests were performed to determine if these vibrations would adversely affect the liquid crystal display. Parallel configuration cells were made and an electrically driven vibrator was constructed. The cell was situated on top of a strip which was set into a bending vibrational mode. The interelectrode spacing of the cell was 50.8μ, the electrodes were evaporated silver and the operating voltage was 20 volts ac. The cells were vibrated for six hours at 56 Hz and six hours at 250 Hz. The amplitude at 56 Hz was 0.16 inch peak to peak and at 250 Hz was 0.12 inch peak to peak. If the vibration is harmonic this corresponds to 2.5g at 56 Hz and 40g at 250 Hz. The military specification for vibration in aircraft is given in Table 5.3. The severity of both tests substantially exceeded the specification. No change was observed in the physical contrast ratio during the tests.

TABLE 5.3

MILITARY SPECIFICATIONS FOR VIBRATIONS IN AIRCRAFT

Frequency Range (Hz)	Amplitude
5 to 10	0.08 inch peak to peak
10 to 14	0.042g
14 to 60	0.036 inch peak to peak
60 to 500	±10g

SECTION 6

BASIC PROPERTIES OF LIQUID CRYSTALS

6.1 Introduction

Several studies were made relating to the basic properties of liquid crystals. The results of these studies are presented in the following sections. The results of the first study (Section 6.2) served to increase our confidence in the existing theories. The results of the second and third studies (Sections 6.3 and 6.4) appear to have practical application in device design and material selection. The results of the fourth study are primarily of interest in basic studies of the scattering mechanism.

6.2 Verification of Heilmeier's Theory of Electrohydrodynamic Instability

Heilmeier has proposed a simple model to predict the threshold of instability in a conducting fluid. He notes that instability should occur if the fluid velocity due to space charge and electric field exceeds the drift velocity of the ions in the conducting fluid. He proposed the following relation:

$$V_{th} = \frac{\eta \mu}{\epsilon \epsilon_0}$$

where V_{th} is the threshold voltage for instability

η is the viscosity of the fluid

μ is the ion mobility

ϵ is the dielectric constant

and ϵ_0 is the permittivity of free space

The product ημ (Walden's constant) does not vary substantially from material to material. The validity of the relationship was tested by measuring the dielectric constant and threshold voltage of a MBBA liquid crystal sample 50.8μ thick. Large changes were induced in the dielectric constant of the liquid crystal by aging the material in a 15 volt dc field. The data obtained are shown in Figure 6.1. The linear variation observed is consistent with Heilmeier's model. A more detailed account of this work has been submitted to Applied Physics Letters. A copy of this manuscript is contained in Appendix E.

6.3 The Effect of Shear on Contrast Ratio

Some theoretical models for dynamic scattering in liquid crystals are based on the premise that turbulence is caused by shear stresses generated by ions in transit in the liquid. Experiments were performed to determine if externally applied shear stresses would induce a turbulent state in a liquid crystal. A sandwich cell comprising Nesa electrodes, 50.8 spacers and MBBA liquid crystal was subjected to large shear strains. The strain was achieved by moving the top plate relative to the bottom plate by hand at a frequency of about 2 Hz. The results are shown in Table 6.1. The contrast ratio is defined as:

$$C.R._{elec.\ driven} = \frac{light\ detector\ voltage\ (V = 0)}{light\ detector\ voltage\ (V = 40v)}$$

and

$$C.R._{not\ elec.\ driven} = \frac{light\ detector\ voltage\ (shear = 0)}{light\ detector\ voltage\ (shear \neq 0)}$$

The shear effects are rather large and could interfere with the operation of the displays; the displays should be designed to eliminate large shear strains.

TABLE 6.1

	Electrically Driven (40 Volts)	Not Electrically Driven
No shear	2.08	1.00
Low amplitude shear -1/4" movement each way	1.66	1.68
Large amplitude shear ~1" movement each way	1.29	2.50

6.4 Birefringence of Liquid Crystals

The contrast ratio obtainable in a nematic liquid crystal device is
primarily dependent on the optical anisotropy of the liquid crystal. The
best measure of this anisotropy is the birefringence, that is, the dif-
ference in the two indices of refraction, Δn, of the uniaxial liquid crystal.
When the liquid crystal is in a turbulent state, an incoming light ray
encounters regions of different molecular orientation and consequently is
scattered. The amount of scattering is directly proportional to the
birefringence. Consequently, the contrast potential of various liquid
crystal materials can be determined independent of the cell geometry
provided the birefringence can be measured.

The wedge technique of Chatelain was used to measure the birefringence
of the available liquid crystal materials. A laser beam was directed through
a wedge of liquid crystal material (Figure 6.2) and the deviation of the two
emerging beams was measured. The liquid crystal was oriented by applying
a magnetic field of 3,000 gauss. The birefringence is determined from the
deviation as indicated on Figure 6.2. Birefringence data for these materials
are shown in Figure 6.3 as a function of temperature. The Merck IV material
has the largest birefringence at room temperature and the variation from
material to material is less than 30%. These data are consistent with con-
trast data taken on operational cells which show only small dependence of
contrast on material. The decrease in birefringence with temperature is
significant since it predicts the device contrast will decrease with
increasing temperature and the device may become inoperable well before the
transition temperature is reached.

6.4 Noise Measurements in Nematic Liquid Crystals

Noise measurements were made to gain a better understanding of the electronic transport mechanism and dynamic scattering process in liquid crystals. The results of this study were reported in a paper to be published in Molecular Crystals and Liquid Crystals. A copy of this paper is included in Appendix F.

SECTION 7

DESIGN CONFIGURATIONS

7.1 System Design

Although the scope of the present program does not specifically include the electronics, consideration must be given to the overall system to preclude the design of an impractical display.

Systems oriented considerations include voltage and power requirements and electronic interconnection requirements. Because of the high impedance of the liquid crystal cell, power requirements are minimal and present no problem.

To minimize the cost of the electronics the display should be voltage compatible with standard digital logic integrated circuits. Since most liquid crystal cells operate at voltages substantially greater than available logic levels designs should be used which minimize voltage requirements.

The display may contain over 100 radial lines. This presents a problem since use of a 100-pin connector is expensive. The use of an expensive connector can be avoided by encoding the selection signals in the off-display electronics and decoding the address on the display. Only seven signal lines are required to address 128 radial line pairs if the decoding is done on the display. If allowance is made for ground and voltage leads an economical ten or twelve pin connector would be adequate. Consequently, the need to include logic circuitry on the display should be considered in the display design.

To be practical the display must be inexpensive and acceptable to the ultimate user. The avoidance of expensive components or processes must be a prime consideration in the design. An acceptable system might comprise a rigid work board 16-by-20 inches in size on which are mounted two radial display devices of nine inch diameter. The mounting would consist of two jointed arms each attached at one end to the center of a radial display and at the other to the work board. The user would slide the folded map under the radial displays and position the radial displays over the appropriate VOR stations. The electrical connections would be carried through the jointed arms to the next level of electronics mounted on the work board. A small light mounted on the board would guarantee a minimum light level. The radial displays need be large enough to span the VOR station locations; the optimum diameter has not been determined, but it should not exceed nine inches.

7.2 Packaging

The details of the packaging problem depend on the configuration used for the liquid crystal cell. For either configuration a top layer is required to confine the liquid crystal and preferably to make a hermetically sealed enclosure. For both configurations a practical method for adding the liquid crystal must be devised.

In the parallel case the top layer must be transparent and electrically conductive. This requirement limits the possible materials to Nesa or Nesatron glass, gold coated glass or gold coated plastic. Only the latter material is flexible and if tests show that it is not stable, only a rigid display may be feasible in this configuration.

In the perpendicular case the top layer must be transparent and electrically insulating. This requirement is met by a large number of materials. The critical spacing is between the electrodes and this dimension is fixed in the relatively controlable etching process. Consequently the perpendicular configuration appears to be more practical for low-cost, high-volume production.

In either configuration a hyperdermic needle may be used to add the liquid crystal after assembly. However, this method does not appear to be a practical approach for a production process. If the liquid crystal is added before the top layer, care must be exercised not to contaminate the sealing surface or to trap air bubbles. Although these problems are formidable, the latter insertion method appears to have the greater promise for a practical production process.

7.3 Geometric Design

7.3.1 Perpendicular Configuration

The test results suggest that the physical contrast ratio obtainable with the perpendicular configuration is not as good as that obtained for the parallel configuration. The packaging of the perpendicular configuration appears to be simpler in that the top cover need not be conductive and the electrode spacing does not depend on the cover. If a usable conductive, flexible, transparent cover cannot be found for use in the parallel configuration, then the perpendicular configuration may be the only way of achieving a flexible display.

The disadvantages of the perpendicular configuration are the high voltage required for operation and the low contrast. The high voltage requirement is due to the wider electrode spacing required in this

configuration. A typical spacing for the parallel configuration is one-half mil. Spacing in the perpendicular case is limited by fabrication processes and visibility considerations. The fabrication limit on electrode spacing depends on the thickness of the conductor which, in this case, is also the optical path length. The optimum optical path length is 1/2 mil and this sets the minimum line spacing at one mil; a more practical limit is 2 mils. Four times the voltage needed to operate a parallel cell would be required to operate a comparable perpendicular cell.

The visibility limitation is demonstrated in Figure 7.1. Sets of parallel lines have been placed over the map to simulate a display. The line widths are 4 mils in all cases and the line separations are 5, 10, 20 and 40 mils. None of the line pairs interfere with the legibility of the map; however, it is clear that if liquid crystal contained between the five-mil spaced lines were activated the line would not be highly visible. Five mil spacing requires a few hundred volts of applied potential for operation. Lines with wider spacing require proportionally higher voltages and are impractical.

7.3.2 Parallel Configuration

The advantages of the parallel configuration are that narrow interelectrode spacing and relatively wide lines are easily attained. The narrow spacing allows the use of relatively low voltage compared to that required in a practical perpendicular geometry. The wide lines provide high visibility without the use of the high resolution patterns which are required in the perpendicular configuration.

The disadvantages of the parallel configuration are in fabrication and in the need for a transparent, electrically conductive top cover. The fabrication problem is in sealing and maintaining proper spacing between the electrodes. Experimental parallel configuration models are actually easier to make than the perpendicular configuration models; however, greater difficulties are anticipated in production.

SECTION 8

FULL SCALE DISPLAY MODEL

8.1 General Description

Two full scale display models were designed: one in the parallel and one in the perpendicular configuration. The displays (Figure 8.1) are nine inches in active area and have ten lines spaced 10° apart in the first quadrant and one or more lines in the other quadrants. The units are intended to have reflective backing behind the lines, and sealable covers.

8.2 Perpendicular Configuration

The perpendicular configuration incorporates a multisegment line and is shown in Figure 8.2. The segments are two mils wide and define 4 two-mil-wide spaces. Additional 3 mil wide copper strips are located on either side of the segments. These strips are used for sealing and to carry the electrical signal. The base is Kapton 2 mils thick and the copper is 1/2 oz. The cover consists of a 3 mil thick nylon base clad with 3 mils of copper. The copper is etched to match the pattern of 3 mil wide lines on the lower segment. In assembly the liquid crystal would be placed (Section 9) in the spaces between the two-mil-wide electrodes. A bead of adhesive would be placed along the outside edges of the three mil wide lines and the cover would be pressed in place. Electrical contact would be made to the protruding 1/4 inch extensions to the 3 mil wide lines. In an operating model (including electronics) these extensions would be on the inner ends of the lines. Two mil wide spaces were chosen as a compromise between manufacturability and voltage requirements. No adhesive layer is permitted between the Kapton and copper as this might

contaminate the liquid crystal. Adhesives may be used on the cover since the adhesive areas should not be in contact with the liquid crystal. The cover has more than two mils of clearance above the liquid crystal and is relatively rigid. It should not touch the liquid crystal when the display is flexed. The reflective backing is located on the bottom of the Kapton base under the line segments. A photograph of the display is shown in Figure 8.3.

8.3 Parallel Configuration

A cross section of parallel configuration line is shown in Figure 8.4. The starting material is 2 mil copper on 1/2 mil Kapton. Adhesive may not be used. The Kapton is etched to form the 15 mil wide line and the exposed copper is electroplated with nickle or chromium to form a highly reflective surface. The copper is then etched to form 30 mil wide lines. The cover consists of 30 mil wide strips of conductive coated, transparent, flexible plastic. These are placed over the copper lines after the cavity has been filled with liquid crystal. A bead of adhesive along the outside edge of the cover seals the system.

SECTION 9

FABRICATION OF DISPLAY MODELS

9.1 General Description

The display models were fabricated by Towne Laboratories of Somerville, New Jersey; the size was too large for the equipment available at Drexel. The only potentially difficult operation was the etching of the Kapton and a suitable process was developed at Drexel with much advise and help from the suppliers. The Kapton etching procedure is described in Appendix G.

9.2 Insertion of Liquid Crystals

One of the early problems in this program was the insertion of the liquid crystal into the narrow lines. If the lines are filled until they overflow, the contrast ratio is observed to decrease and the liquid crystal contaminates the sealing areas. The liquid crystals are now inserted by using a one microliter capacity syringe fitted with a dispenser which releases 1/50 of the syringe capacity each time it is operated. This device is mounted on a projected microscope so that the filling operation can be observed at 40 power. Use of this equipment allows close control of the filling operation and has essentially solved this problem.

9.3 Cleaning Procedure

The cleaning cycle has been improved and modified. All work is now being done under a hood and particular care is taken to clean the cells as well as possible without leaving any chemical residue which might interact with the liquid crystal.

A typical cycle is:

1. Freon T-p35 solvent is sprayed on the cell with a MS-226 Cobra extension nozzle. The nozzle makes it possible to pin-point a fine stream of the solvent onto the cell pattern in order to clean away dust and dirt. Freon T-p35 solvent is a blend of Freon TF and isopropyl alcohol.

2. Next the cell is scrubbed with a foam swab soaked with isopropyl alcohol. The foam swab is made by Texwipe and is totally lint-free for non-contaminative cleaning.

3. The cell is sprayed again with Freon T-p35 and transferred to a degreaser filled with isopropyl alcohol.

4. A can of MS-220 clean air is used after the cleaning cycle for drying the cell.

SECTION 10

EVALUATION OF DISPLAY MODELS

A number of problems have been encountered with the display models; some are due to poor technique and others are fundamental.

In the fundamental class is the sealing of the cover to the parallel configuration display. When the cover is placed on the display, capillary forces draw the liquid crystal material out from the channel and they contaminate the seal area (as well as deplete the channel). The approach being tried to circumvent this problem is to freeze the liquid crystal after it is inserted and to seal the cover in place while the crystal is frozen. On thawing the crystal may "wick-out" to the sealing material, but the contact will be over a minimal area and some of the newer silicons apparently do not interact with the crystal material.

Another fundamental problem is the "puckering" of the Kapton in the parallel configuration case. This "puckering" is apparently due to stresses in the copper and can presumably be eliminated by obtaining a stress free copper.

In the poor technique class is the residue left on the bottom of the Kapton channel. This is due to the repolymerization of the Kapton after etching and can be controled by proper etching technique. Other problems include shorts in the perpendicular configuration lines, nodules on the perpendicular lines which cause premature voltage breakdown and some peeling of the etched copper lines. All of these problems can be solved by use of proper techniques.

SECTION 11

DEMONSTRATION MODEL

A demonstration model comprising a non-operating, full-size

perpendicular configuration display and a fully operational, sealed,

perpendicular-configuration (4 inches long) line will be submitted to

NASA in February 1972. The problems with Kapton residue, puckering and

sealing, prevent the submission of a parallel configuration display.

SECTION 12

CONCLUSIONS

Significant progress has been made toward the development of a practical liquid crystal display system for use in air navigation. Sufficient data have been generated and materials obtained to fabricate a full-scale device of at least marginal quality at this time. Several techniques for fabricating substantially improved devices are being evaluated under the continuation grant. Areas requiring improvement include contrast and operating voltage. Both appear to depend on the purity of the liquid crystal. Contrast depends, in addition, on the materials and methods of fabrication.

Sufficient progress has been made to make it desirable to incorporate the electronic design limitations into the system design; this is presently being done under the continuation grant.

SECTION 13

BIBLIOGRAPHY

1. "Dynamic Scattering: A New Electro-optic Effect in Certain
   Classes of Nematic Liquid Crystals," Heilmeiser, Zanoni and
   Barton, Proceedings IEEE, Vol. 56, No. 7, p. 1162 (July 1968).

2. "Note on Transient Current Measurements in Liquid Crystals and
   Related Systems," Heilmeier and Heyman, Physical Review Letters,
   Vol. 18, No. 15, p. 583 (10 April 1967).

3. "Transient Behavior of Domains in Liquid Crystals," Heilmeier,
   Journal of Chemical Physics, Vol. 44, No. 2, p. 644 (1966).

4. "Orientational Oscillations in Nematic Liquid Crystals," Heilmeier
   and Helfrich, Applied Physics Letters, Vol. 16, No. 4, p. 155
   (February 1970).

5. "Possible Ferroelectric Effects in Liquid Crystals and Related
   Liquids," Williams and Heilmeier, Journal of Chem. Physics,
   Vol. 44, No. 2, p. 638 (January 1966).

6. "Liquid Crystal Display Devices," Heilmeier, Scientific American,
   Vol. 222, p. 100 (1970).

7. "Further Studies of the Dynamic Scattering Mode in Nematic Liquid
   Crystals," Heilmeier, Zanoni and Burton, IEEE Transactions on
   Electron Devices, Vol. ED17, No. 1, p. 22 (January 1970).

8. "A Simplified Electrohydrodynamic Treatment of Threshold Effects
   in Nematic Liquid Crystals," Heilmeier, Proceedings IEEE, Vol. 59,
   No. 3, p. 422 (March 1971).

9. "Anisotropic Ultrasonic Properties of a Nematic Liquid Crystal,"
   Lord and Labes, Physical Review Letters, Vol. 25, No. 9, p. 570
   (August 1970).

10. "Liquid Crystals," Fergason, Scientific American, p. 77 (1964).

11. "Cholestric Liquid Crystals for Optical Applications," Kahn, Applied
    Physical Letters, Vol. 18, No. 6, p. 231 (15 March 1971).

12. "Behavior of Anisotropic Liquids in an Electric Field," Soviet
    Physics, Vol. 9, p. 235 (1964).

13. "Reflective Liquid Crystal Television Display," John A. Realte,
    Proceedings IEEE, Vol. 5, No. 12, p. 2147 (1968).

14. "Light Deflection Phenomena in an AC Excited Nematic Liquid Crystal
    Sample," Sun Lu and Derrick Jones, Journal of Applied Physics, Vol. 42,
    p. 2138 (1971).

15. "Electrically Scanned Analog Liquid Crystal Displays," Soref,
    Applied Optics, Vol. 9, No. 6, p. 1323 (1970).

16. "Reversible Ultrasonic Imaging with Liquid Crystals," Margreum,
    Nimoy and Young, Applied Physics Letters, Vol. 17, No. 2, p. 51
    (1970).

17. "Dynamic Scattering in Room-Temp. Nematic Liquid Crystal,"
    Derrick Jones, Linda Creigh and Sun Lu, Applied Physics Letters,
    Vol. 16, No. 2, p. 61 (1969).

18. "Electrical Field Distribution Associated with Dynamic Scattering
    in Nematic Liquid Crystals," Sun Lu and Derrick Jones, Applied
    Physics Letters, Vol. 16, No.12, p. 484 (1969).

19. "Electrophotographic Imaging with Cholesteric Liquid Crystals,"
    Haas and Adams, Applied Optics, Vol. 7, No. 6, p. 1203 (1968).

20. "Electric Field Hysterisis Effects in Cholesteric Liquid Crystals,"
    Melamed and Rubin, Applied Physics Letters, Vol. 16, No. 4, p. 149
    (1969).

21. "Voltage Induced Vorticity and Optical Focusing in Liquid Crystals,"
    Penz, Physical Review Letters, Vol. 24, No. 25, p. 1405 (1970).

22. "New Electro Optic Effect in a Room Temperature Nematic Liquid
    Crystals," Haas, Adams and Elannery, Physical Review Letters,
    Vol. 25, No. 19, p. 1325 (1970).

23. "Temperature Dependence of Birefringence in Liquid Crystals,
    Balzaini, Physical Review Letters, p. 914 (October 1970).

24. "Hydrodynamic Instabilities in Nematic Liquids Under AC Electric
    Fields," Orsay Liquid Crystal Group, Physical Review Letters,
    Vol. 25, p. 1642 (December 1970).

25. "Experiment with Cholesteric Liquid Crystals," Fergason, American
    Journal of Physics, Vol. 38, No. 4, p. 425 (1970).

26. "Scattering of Coherent Light from Nematic Liquid Crystals in
    Dynamic Mode," Journal of Applied Physics, Vol. 40, No. 10, p. 4049
    (1970).

27. "Optical Contrast Enhancement in Liquid Crystal Devices by Spatial
    Filtering," Applied Physics Letters, Vol. 18, No. 1, p. 5 (1971).

28. "Current and Magnetic Field Induced Order and Disorder in Ordered
    Nematic Liquid Crystals," Teany and Migim, Journal of Applied Physics,
    Vol. 41, No. 3, p. 998 (1969).

29. "The Physics and Chemistry of Liquid Crystals," Soref, SID Digest, p. 122 (May 1971).

30. "Light Scattering in Electric Field Devices Nematic Liquid Crystals," Goodman, SID, p. 124 (May 1971).

31. "Transient Scattering of Light by Pulsed Liquid Crystal Cells," L.S. Cosentino, SID, p. 126 (May 1971).

32. "MOS Driven Liquid Crystal Display," Bosell and Robert, SID, p. 128 (May 1971).

33. "Cholestric Nematic Phase Transition Displays," Wysocki, et al, SID, p. 130 (May 1971).

34. "Nematic Liquid Crystals - Cinemicerography of Electrohydiodynamic Instabilities," Kashnow, SID, p. 134 (May 1971).

35. "Guest Host Interactions in Nematic Liquid Crystals - A New Electro Optic Effect," Heilmeier and L. A. Zanoni, Applied Physics Letters, Vol. 13, No. 3, p. 91 (1968).

36. "Solid Facts about Liquid Crystals," R. A. Soref, Laser Focus, p. 45 (September 1970).

37. "Now That the Heat Is Off, Liquid Crystals Can Show Their Colors Everywhere," Joseph Castellano, Electronics, (July 6, 1970).

38. "Electrohydrodynamic Instabilities in Nematic Liquid Crystals," W. H. DeJeu, C. J. Gerritsma and Van Boster, Physics Letters, Vol. 34A, No. 4, p. 203 (8 March 1971).

39. "Performance Characteristics of Nematic Liquid Crystal Display Devices," L.T. Creagh, A.R. Kinetz, and R.A. Reynolds, IEEE Trans. on Electron Devices, Vol ED-18, No. 9, pp. 672-678, (September 1971).

40. "Deformation of Nematic Liquid Crystals with Vertical Orientation in Electric Fields," M.F. Schiekel and K. Fahrenschon, Appl. Phys. Letters, Vol. 19, pp. 391-393, (1971).

41. "Effects of Additions of Cholesterics on Nematic Liquid Crystal Properties," B. Kerllenevich and A. Coche, J. Appl. Phys., Vol. 42, pp.5313-5315, (1971).

42. "Electrically Controlable Domains in Nematic Liquid Crystals," W. Greubel and V. Wolff, Appl. Phys. Letters, Vol. 19, pp. 213-215 (1971).

43. "Effects of Dopants on Display Characteristics of the Nematic 4-Methoxy-benzylidence-4-Buttaniline," Linda T. Creagh and Allan R. Kinetz, Meeting Abstracts-ACS Meeting, Wash., D.C. (September 1971).

44. "Dielectric and Resistivity Measurements on Room Temperature Nematic MBBA, F. Rondelez, D. Diquet, and G. Durand, Mol. Cryst. and Liq. Cryst., Vol. 15, pp. 183-188 (1971).

APPENDIX A

Personnel Assigned to Program

Name	Title	Fraction of Time	
		Academic Year	Summer
* T. J. Matcovich	Professor	1/8	1/14
P. Herczfeld	Assoc. Professor	1/8	1/4
A. Lord	Assoc. Professor	1/8	1/2
J. Wargin	Research Assistant	** 1	1
F. Wargocky	Research Assistant	1	1
W. DaCosta	Research Assistant	1	1
Z. Turski	Research Assistant	*** Part Time	0

*   Principal Investigator

**   2/3 Time in Winter and Spring Quarters

***   Winter and Spring Quarters Only

APPENDIX B

SEMINARS AND CONFERENCES

Seminars at Drexel University

"Effect on Electrical and Optical Properties of Field Induced Orientation
in Nematic and Cholesteric Liquid Crystals"

Dr. Alan Sussman
RCA Princeton Laboratories

May 12, 1971 - Stratton Hall

"Some Recent Advances in Liquid Crystals"

Dr. James E. Adams
Xerox Corporation, Rochester, New York

June 2, 1971 - Stratton Hall

Conferences

1970 IEEE Conference on Display Devices, December 2-3, 1970, New York,
New York.

Attended by Dr. P. Herczfeld

Georgetown Liquid Crystal Symposium, May 2, 1971, Washington, D.C.

Attended by Dr. A. Lord

1971 SID Conference, May 4-6, 1971, Philadelphia, Pennsylvania

Attended by Dr. T. J. Matcovich

APPENDIX C

Commercially Available Room Temperature Nematics

Eastman Organic Chemicals Rochester, New York	10 - 41°C 5 - 105°C	MBBA No. 11246 *MBBA No. 11643
Liquid Crystal Industries 460 Brown Avenue Turtle Creek, Pennsylvania	18 - 80°C	Nematic Liquid Crystal
Vari-Light Corporation 9770 Cronklin Road Cincinnati, Ohio	10 - 47°C	VL 462N
EM Laboratories 500 Executive Avenue Elmsford, New York	16 - 60°C -5 - 75°C	Merck, Licristal IV *Merck Licristal V

*newly available materials

APPENDIX D

PARTIAL LIST OF SUPPLIES

Photoresists, Developer:
  Shipley Company, Inc. - Newton, Massachusetts

Al Etchant:
  Transene Company - Rowley, Massachusetts

Cu Plating bath:
  Sel - Rex Company, Meaker Division - Nutley, New Jersey

Cu Etchant:
  MacDermid, Inc. - Waterbury, Connecticut

Filters for Resist:
  Millipore Corporation - Bedford Massachusetts

Adhesive/Sealant
  Dow Corning Corporation - Midland, Michigan

Masks, Etching of Cu-slides, Etching of Prototypes:
  Towne Laboratories Inc. - Somerville, New Jersey

Cleaning Detergent:
  Ultrasonic Industries - Hicksville, Long Island, New York

Syringes, Dispenser
  Hamilton Company - Whittier, California

Foam Swabs
  Texwipe Company - Hilldale, New Jersey

Freon and Cleaners
  Miller-Stephenson Chemical Company, Dansbury, Connecticut

APPENDIX E

VARIATION OF DC DOMAIN THRESHOLD IN A NEMATIC LIQUID CRYSTAL DUE TO CHANGES IN DIELECTRIC CONSTANT

A copy of this paper is presented in the following pages. This paper has been submitted for publication to Applied Physics Letters.

APPENDIX F

NOISE MEASUREMENTS IN NEMATIC LIQUID CRYSTALS

A copy of this paper is presented in the following pages. This paper has been accepted for publication in Molecular Crystals and Liquid Crystals.

VARIATION OF DC DOMAIN THRESHOLD IN A NEMATIC LIQUID
CRYSTAL DUE TO CHANGES IN DIELECTRIC CONSTANT*

by

F.E. Wargocki and A.E. Lord, Jr

Physics Department
Drexel University
Philadelphia, Pennsylvania 19104

Changes have been observed in several properties of nematic liquid crystals during continual dynamic scattering under DC fields (henceforth called aging). With time, a significant change in nematic-isotropic transition temperature, conductivity and dielectric constant can be induced under relatively small DC voltages. Several 50.6µm thick sandwich cells of MBBA with NESA electrodes have been run under 15 volt DC voltages and the threshold voltage (DC) for domain formation, cell capacitance and conductivity measured against cell age. The results for a representative cell are seen in Figure 1, which is a plot of threshold voltage vs C^{-1}, where C is the cell capacitance measured at 1 KHz, perpendicular to an orienting magnetic field of 5 KG. A similar plot is obtained with the capacitance measured parallel to the orienting field. The point laying off the straight line represents data taken on the cell before aging, and this behavior is reproducible among our cells, but is yet unexplained.

DeGennes[1] has recently proposed a model for the cellular motion in nematics which combined the effects of convective flow due to strong unipolar charge injection (the Felici instability[2]), dielectric relaxation, elastic restoring torque, and conduction induced torque (the Carr-Helfrich effect[3]). His result is that the voltage at which cellular flow begins, V_c, is given by

$$\frac{V_c}{V_i} = 1 - \frac{\lambda \, V_c^2}{V_c + V_0^2}$$

where

$$V_1 = 16\pi^2 \frac{\mu\eta}{\epsilon\epsilon_0}$$

$$\lambda = \frac{\sigma_a}{4\sigma}\left[1 + \frac{\gamma_1}{|\epsilon_a|\eta}\right]$$

and

V_0 is a constant, typically a few volts

μ is the average mobility of the injected carriers

η is an average viscosity

γ_1 is a shear-torque coefficient

ϵ is the dielectric constant

$\epsilon_a = \epsilon_\perp - \epsilon_{||}$, the dielectric anisotropy

σ is the conductivity

$\sigma_a = \sigma_\perp - \sigma_{||}$, the conductivity anisotropy.

V_1 is the threshold voltage for cellular currents due to the Felici instability alone and calculated by Atten and Moreau[4] for the case of strong unipolar injection. When $\lambda > 1$ the threshold is dominated by the Carr-Helfrich effect; when $\lambda < 1$ this effect is diminished and the threshold is dominated by the Felici instability.

The measured average conductivity of our material was $3 \times 10^{-10}(\Omega\cdot\text{cm})^{-1}$ and the average conductivity anisotropy was $1.1 \times 10^{-10}(\Omega\cdot\text{cm})^{-1}$. The average

dielectric anisotropy was 0.8. Using deGennes' value of $\gamma_1/\eta = 2.5$ for MBBA[5], we can calculate $\lambda = 0.35$. Due to variations in the conductivity and anisotropy during aging, λ varied by about 50%. The above test, then, was conducted in the range $\lambda < 1$, where the Felici instability can be expected to dominate and the threshold should vary linearly with ε^{-1}. Our results confirm this.

Heilmeier[6] has proposed a simplified electrohydrodynamic treatment of threshold effects in nematic liquids in which he predicts instability if the drift velocity of an ion in transit exceeds the fluid velocity of the medium, that is, if the counterflow of the fluid is unable to keep up with ion flow. He gives the threshold as

$$V = \frac{\mu\eta}{\varepsilon\varepsilon_0}$$

using the above notation. He too, predicts the $V \sim \varepsilon^{-1}$ behavior that we have observed.

A least squares fit to the data of Figure 1 gives a slope of 4.97×10^{-9} V·F, and considering cell geometry (12 cm² by 50.6μm), this yields a value

$$\mu\eta = 2.1 \times 10^{-10} \text{ Coul·m}^{-1}$$

which is near the value of $1.2-3 \times 10^{-10}$ which Heilmeier gives for PAA[7]. This quantity is known as Walden's constant and for a given electrolyte it varies little for various solvents[8]. Using a value $\eta = 5.6 \times 10^{-2}$ kg/m·s

for MBBA[9], we obtain a mobility $\mu = 3.74 \times 10^{-9}$ $m^2/v \cdot s$ which agrees with a measured value of 10^{-9} $m^2/v \cdot s$[10].

There is a functional similarity between Heilmeier's result and Atten and Moreau's expression for V_i, however they differ by the factor $16\pi^2$, a factor we have not been able to reconcile as yet*.

Our results help confirm the general ideas of deGennes and Heilmeier concerning the electrohydrodynamic instability. It also appears that the aging treatment approach will allow a direct determination of Walden's constant which, in turn, allows a determination of either the viscosity or mobility value if the other one is known. If both are known it serves as an independent verification.

*Schneider and Watson[11] have made a similar calculation of threshold voltage for charge injection induced cellular flow in dielectric liquids and they give

$$V \geq 99 \frac{\mu\eta}{\varepsilon\varepsilon_0}$$

so that, in general, these models produce a threshold

$$V = R \frac{\mu\eta}{\varepsilon\varepsilon_0}$$

where R is a criterion of stability analogous to the Rayleigh number in hydrodynamics.

REFERENCES

1. P.G. deGennes, Comments on Solid State Physics $\underline{3}$, 35(1970); $\underline{3}$, 148(1971).

2. N. Felici, Revue Generale d'Electricite $\underline{78}$, 717(1969).

3. W.Helfrich, J. Chem. Phys. $\underline{51}$, 4092(1969).

4. P. Atten and R. Moreau, C.R. Acad. Sc. Paris $\underline{269A}$, 433(1969); $\underline{270A}$, 415(1970).

5. E. Dubois-Violette, P.G. DeGennes, and O. Parodi, J. de Physique $\underline{32}$, 305(1971).

6. G. Heilmeier, Proc. IEEE $\underline{59}$, 422(1971).

7. Heilmeier gives this value as $1.2-3 \times 10^{-12}$. Using his given values for μ and η, however, yields $1.2-3 \times 10^{-10}$(MKS).

8. A.J. Rutgers, Physical Chemistry (Interscience, New York, 1954), p. 338.

9. Ch. Gahwiller, Physics Letters $\underline{36A}$, 311(1971).

10. Orsay Liquid Crystal Group, Proc. 3rd Int. Conf. on Liquid Crystals, (to be published).

11. J. Schneider and P. Watson, The Physics of Fluids $\underline{13}$, 1948(1970).

Noise Measurements in Nematic Liquid Crystals

P. R. Herczfeld and J. T. Hartman
Electrical Engineering Department
Drexel University
Philadelphia, Pennsylvania 19104

Abstract

Experimental results of noise measurements in nematic liquid crystals are presented. The current noise spectra suggest the presence of generation-recombination and diffusion processes in liquid crystal sandwiches. The fluctuation of the photon field, which was transmitted through a liquid crystal sample, was also measured.

Introduction

Transport phenomena and electronic and scattering processes in solid and liquid state materials and devices can be studied in a very meaningful way by fluctuation theory and noise measurements[1,2]. It has been found by many authors that carrier fluctuation, for example in semiconductors, reflect the nature of the fundamental electronic processes and carrier transport present in these crystals. The theory concerns itself with the instantaneous fluctuations in the free carrier densities (n,p), which are related to the voltage and current fluctuation measurements.

The analysis consists of the comparison of the theoretical and experimental curves. The shape of the noise spectra is especially indicative of the fundamental processes involved in the solid. In particular, the theory predicts the high frequency limit of the current noise spectra in solids; some of the representative samples are listed below together with their characteristic high frequency dependence:

i) generation-recombination (g-r) noise $\qquad \omega^{-2}$

ii) diffusion noise $\qquad \omega^{-3/2}$

iii) drift noise $\qquad \omega^{-2}\sin^2\omega\tau_v$

where ω is the angular frequency, τ is bulk recombination lifetime, and τ_v is the drift or transit time.

This paper presents results of experimental noise measurements in nematic liquid crystals. The purpose of these experiments was to gain a better understanding of the electronic transport mechanism and dynamic scattering process in liquid crystals. We were particularly interested in determining if any correlation existed between the current noise in the liquid crystal sandwich and the fluctuation in the transmitted photon field.

Experimental Setup

The block diagram of the experimental apparatus is shown in Fig. 1. The liquid crystal sample consisted of two transparent electrodes separated by a six micron mylar spacer. A circular hole of 1/2 cm in diameter was cut into the spacer material, and the hole was filled with liquid crystal (Merk IV) having a resistivity of 8×10^9 ohm-cm. The light, from a

tungsten filament lamp, was focused on the liquid crystal, and the
non-active area was shielded from the light by an aperture. This
arrangement assured that (i) all the transmitted light pass through
the sample and (ii) the entire sample was illuminated uniformly. The
detector was mounted above the crystal at an angle θ with respect to
the normal, however all the results presented here were made with $\theta=0$.

The liquid crystal was driven by dry batteries, and it showed
excellent ohmic behavior. The light source was also powered by batteries
to minimize the fluctuations in the incident photon field. The trans-
mitted light was detected by a solid state photodetector having a very
low noise characteristic and a linear time response, up to several MHz.
The noise measuring apparatus consisted of a low noise PAR 113 preampli-
fier, a PAR 110 tuned amplifier and a square-law detector.

Measurements and Results

First, the noise spectra of the liquid crystal current fluctuations
(ΔI) were measured at several bias voltages and plotted in relative units
(Figs. 2a, b, and c). Following these, the power spectra of the trans-
mitted photon field fluctuations (ΔJ), as detected by the photodetector,
were measured at the same bias voltages, Figs. 3a and b. It is important
to note that for all these measurements the noise was much above the back-
ground noise. The background noise is defined as the measured noise with
zero bias voltage across the liquid crystal sample; and it includes
the incident photon field fluctuation (white noise), the detector noise
and noise of the entire measuring apparatus. Finally, the noise power
of the crystal current noise (ΔI) and photon fluctuations (ΔJ) were
measured as a function of applied potential at several frequencies (Fig.4).

At low bias voltages, before dynamic scattering sets in, the current noise spectrum has an $\omega^{-3/2}$ slope and a low frequency turnover (Fig. 2a). This kind of noise spectra, in solids, is usually associated with the composite of generation-recombination (g-r) and diffusion processes[2,3]. At 10 volts considerable dynamic scattering is observed. The spectrum has an $(1 + \omega^2 \tau^2)^{-1}$ dependence below 100 Hz, suggesting pure g-r processes (Fig. 2b). Above 100 Hz diffusion dominates ($\omega^{-3/2}$ slope). At 20 volts very strong scattering takes place; the low frequency spectra has a slope somewhere between $\omega^{-5/2}$ and ω^{-3} (Fig. 2c) which, we believe, has not been observed in solids. Once again the high frequency limit indicates diffusion. The relaxation time, τ, can be calculated from the turnovers; its approximate value is 100 milliseconds.

The power spectra of the photon fluctuations drops off very rapidly, its slope is steeper than $\omega^{-5/2}$ (Fig. 3). This kind of spectrum, which is definitely the result of the interaction of the photons with the liquid crystal, has not been observed in the literature.

The noise power of the current fluctuation and transmitted photon fluctuations as a function of the bias potential are plotted, in normalized units, on Fig. 4. The current noise increases sharply with increasing potential, and the photon fluctuation seems to follow the increase of the current fluctuations up to 15 volts, showing certain correlation. However, the photon fluctuations, at 1 Hz and 10 Hz seem, to decrease above 15 volts, i.e., when dynamic scattering becomes very pronounced. It should be noted that the transmitted d. c. light intensity, as detected by the photodetector , was maintained constant at all times by adjusting the incident light intensity. This adjustment compensated for the possible decrease of the transmitted light intensity caused by the angular distribution of the light scattering which is of course a function of the bias

voltage. The angular orientation ($\theta \neq 0$) seemed to have no appreciable effect on the results.

References

1. A. van der Ziel, Fluctuation Phenomena in Semiconductors, Butterworths, 1959.

2. K.M. van Vliet and J. R. Fassett in Fluctuation Phenomena in Solids, (R. E. Burgess, Ed.), p. 268, Academic Press (1965).

3. P. R. Herczfeld and K. M. van Vliet, "Electronic Processes and Fluctuations in Optically Quenched CdS and CdSe Crystals," Physica Status Solidi 27, 681 (1968).

Figure 1.   Block diagram of experimental set up. The incident light is
             normal to the sample.

Figure 2.   Spectral density of current noise in the nematic liquid
             crystal sample at several bias voltages: a - 5 volts,
             b - 10 volts, c - 20 volts.

Figure 3.   Spectral density of photon fluctuations transmitted through
             the liquid crystal with :   a - 10 volts, b - 20 volts,
             bias voltage on the sample.

Figure 4.   Noise power of current fluctuations and photon fluctuations
             per unit bandwidth in relative units. Curves a, b, and c
             correspond to the variance of the current fluctuations at
             1 Hz, 10 Hz, and 100 Hz respectively. Curves d, e, and f
             correspond to the variance of the normalized photon fluctu-
             ations at 1 Hz, 10 Hz, and 100 Hz respectively.
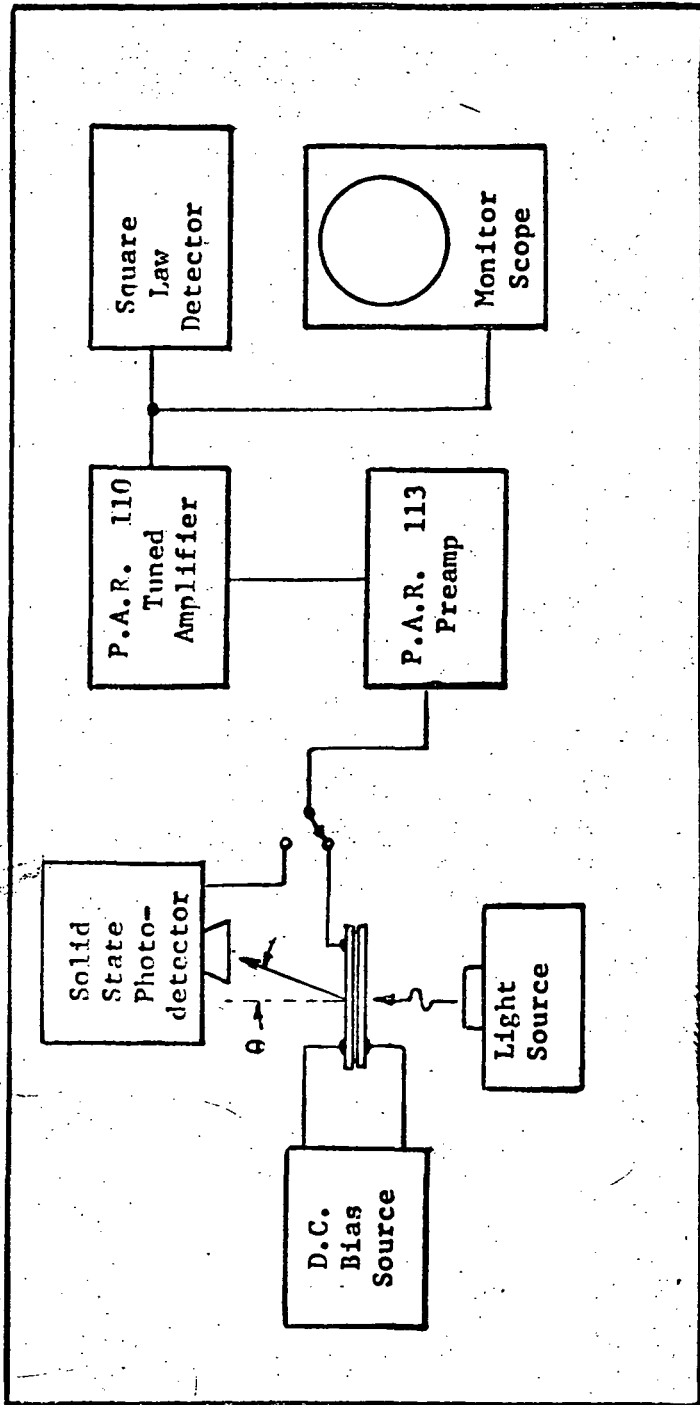
Figure 1
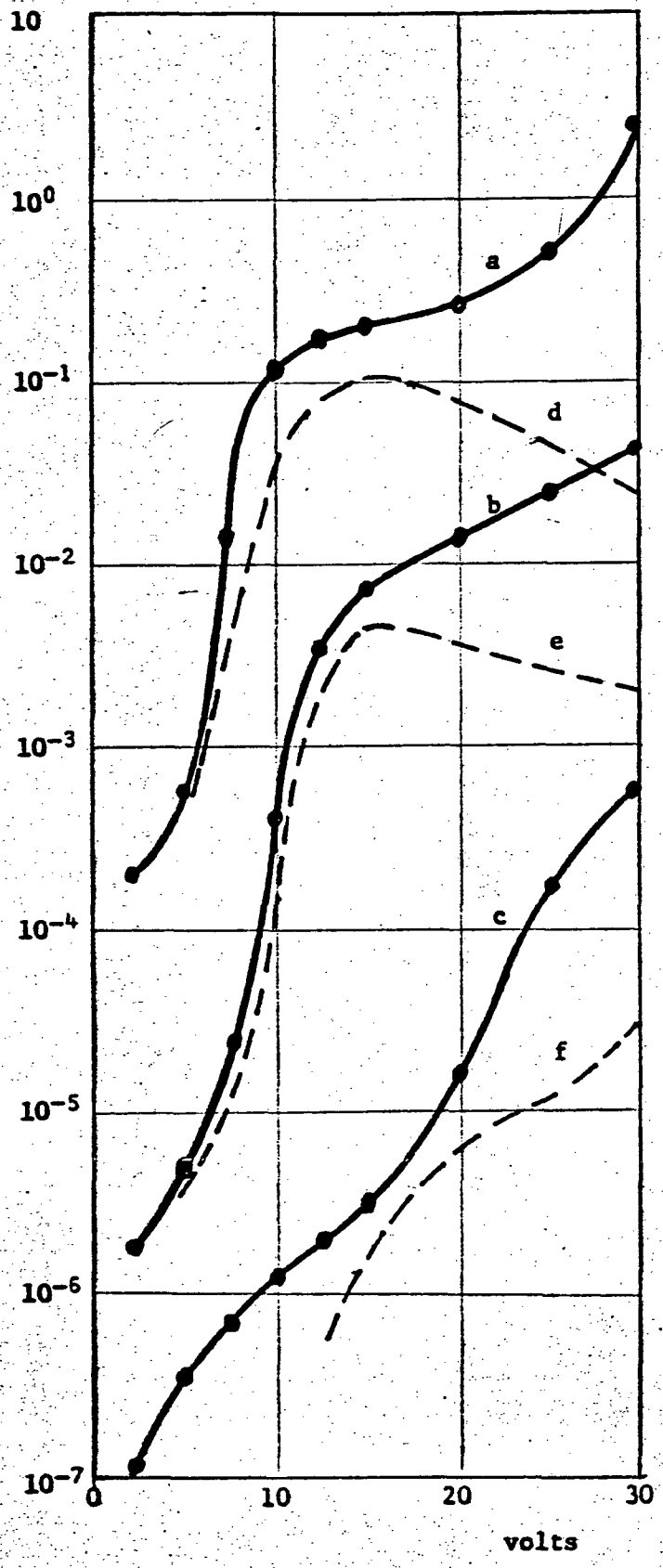
Figure 2

Figure 3

Figure 4

APPENDIX G

KAPTON ETCHING

A narrow channel must be etched in Kapton to fabricate the parallel configuration model described in Section 8. The following procedure was developed in cooperation with a number of suppliers.

A channel to be etched was masked by photoresist. A strong bond between photoresist and Kapton was essential because of the high strength of the etchant. Two layers of KMER were used and, with the cycle described below, the pin-hole density was small.

KMER Cycle:

1. Clean
2. Bake: 1 hour at 200°C
3. Mix KMER: 70% vol. - resist
              30% vol. - thinner
   and apply with the photoresist spinner slide stationary.
4. Spin at 4000 rpm
5. Prebake at 80°C for 1/2 hour
6. Expose
7. Develop according to a procedure described by Westinghouse:
   (a) Spray with KMER developer for 30 seconds--air
       pressure 40 lb., distance 4 in.
   (b) Spray rinse with 80% isopropyl alcohol
       20% KMER thinner for 15 seconds and blow dry
8. Post-bake 1 hour at 150°C min.

To obtain two layers of KMER, repeat points 3, 4, 5 after prebaking the first layer.

The KMER resist comes off very easily with CB-XNT stripper made by Allied Chemical Corporation, Specialty Chemicals Division, Morristown, New Jersey.

The etchant used was: 50% vol. NaOH pellets

50% vol. distilled water.

At a temperature between 100°C and 110°C the etching rate was approximately 1 mil/min: the temperature was very critical.   After etching the sample should not be allowed to dry.   Following the etching, spray the sample with water at room temperature and high pressure for five minutes.   Then put the sample into a mild solution of HCl or other acid.

TRANSPARENT
SUBSTRATE

LIQUID CRYSTAL

CONDUCTORS
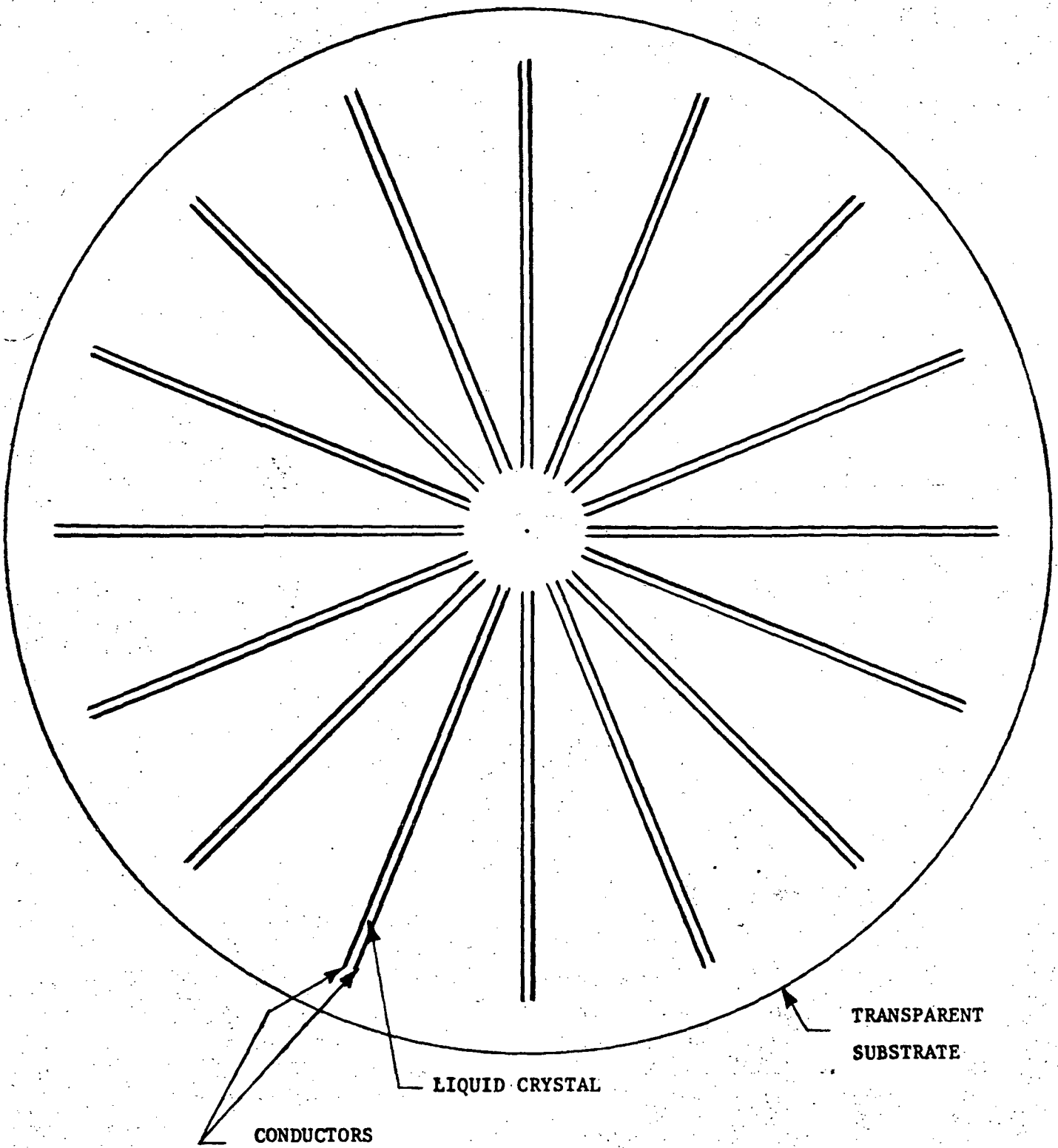
Figure 1.1

DISPLAY PATTERN

PARALLEL CONFIGURATION

TRANSPARENT
ELECTRODES

$\bar{E}$

LIQUID CRYSTAL

LIGHT BEAM
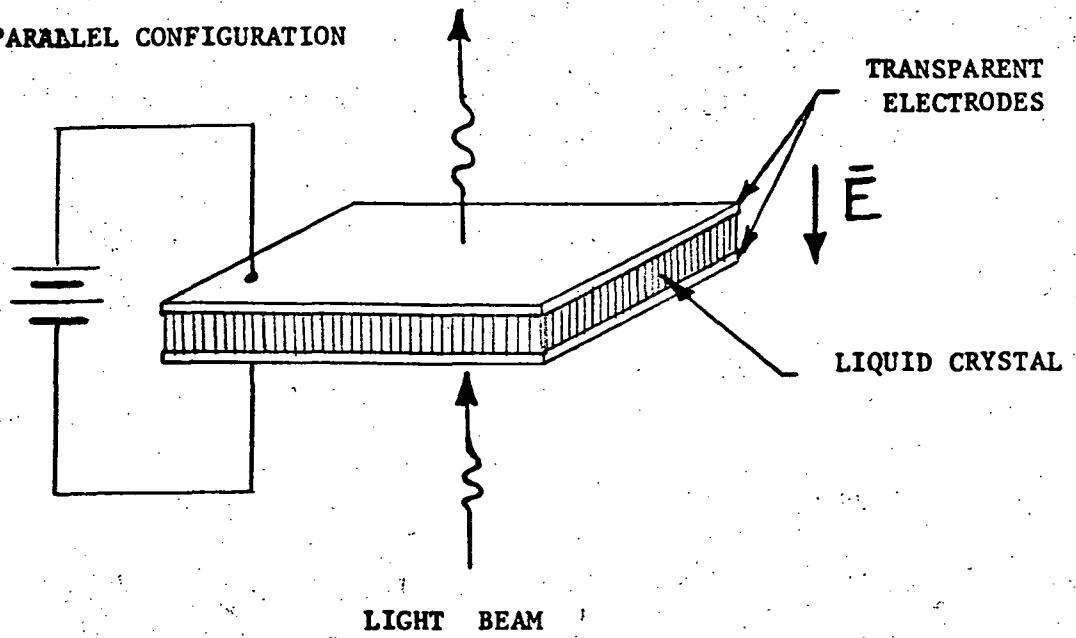
Figure 2.1a

PERPENDICULAR CONFIGURATION

$\bar{E}$

ELECTRODES
LIQUID CRYSTAL

LIGHT BEAM
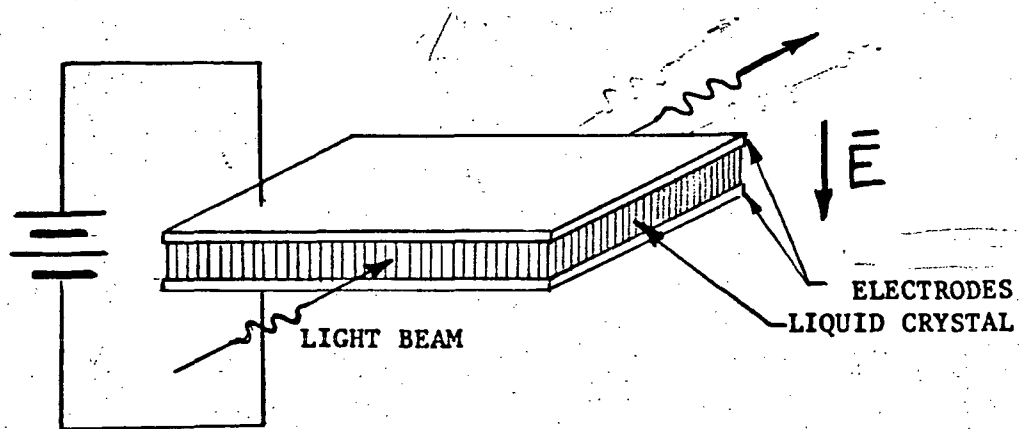
Figure 2.1b

BASIC CELL CONFIGURATIONS

TRANSPARENT TOP COVER

LIQUID CRYSTAL

KAPTON

CONDUCTORS

KAPTON
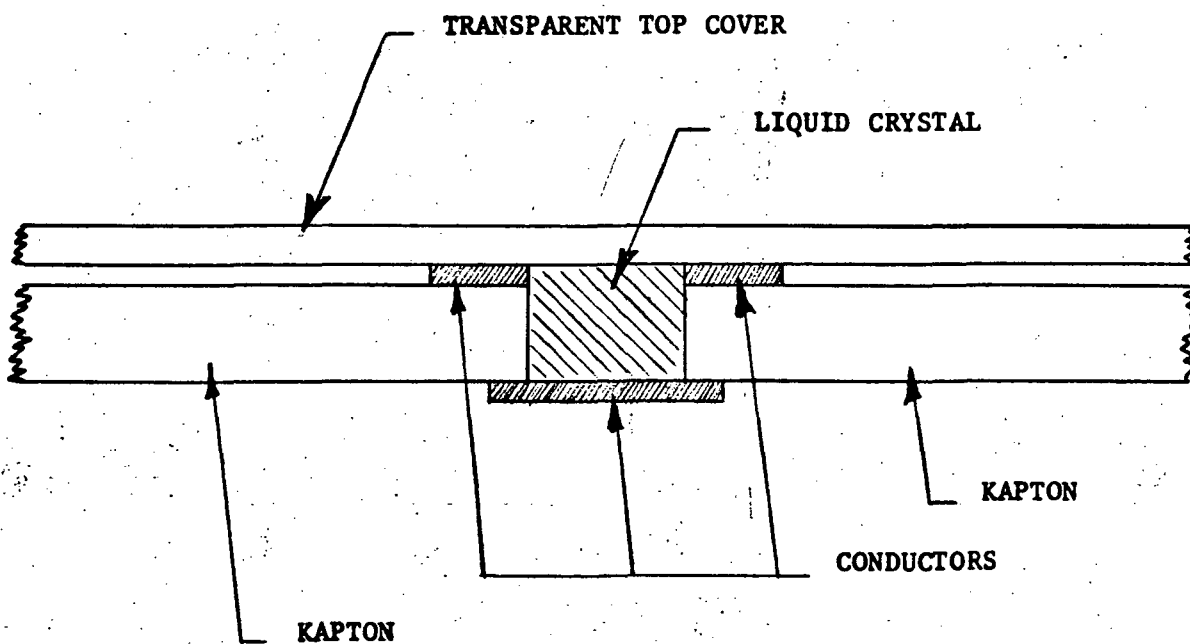
Figure 2.2

EDGE CONFIGURATION
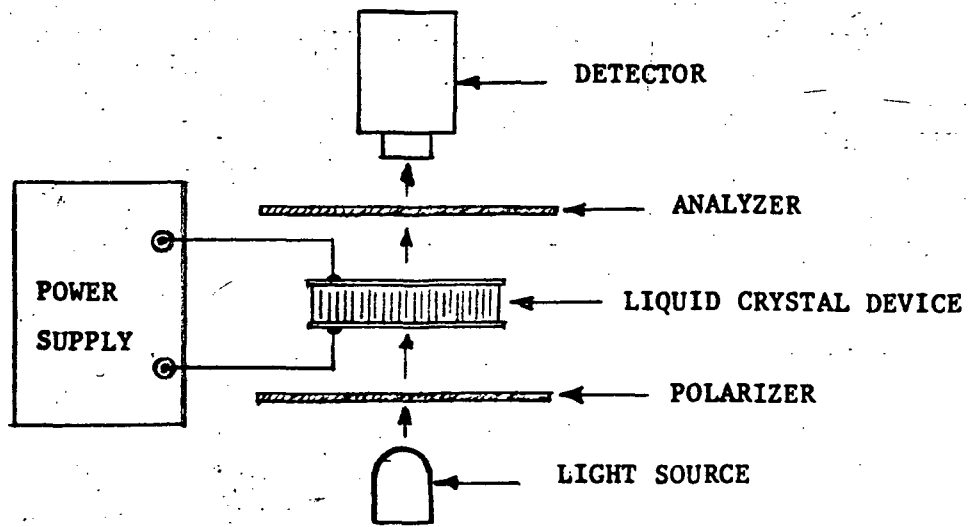
Figure 4.1a
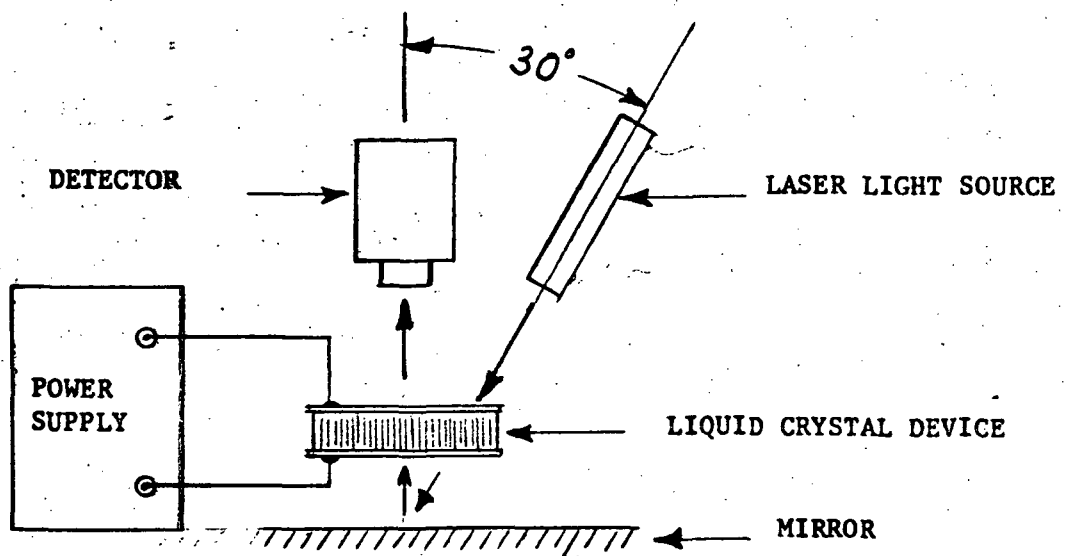
Figure 4.1b

APPARATUS FOR MEASURING CONTRAST RATIO
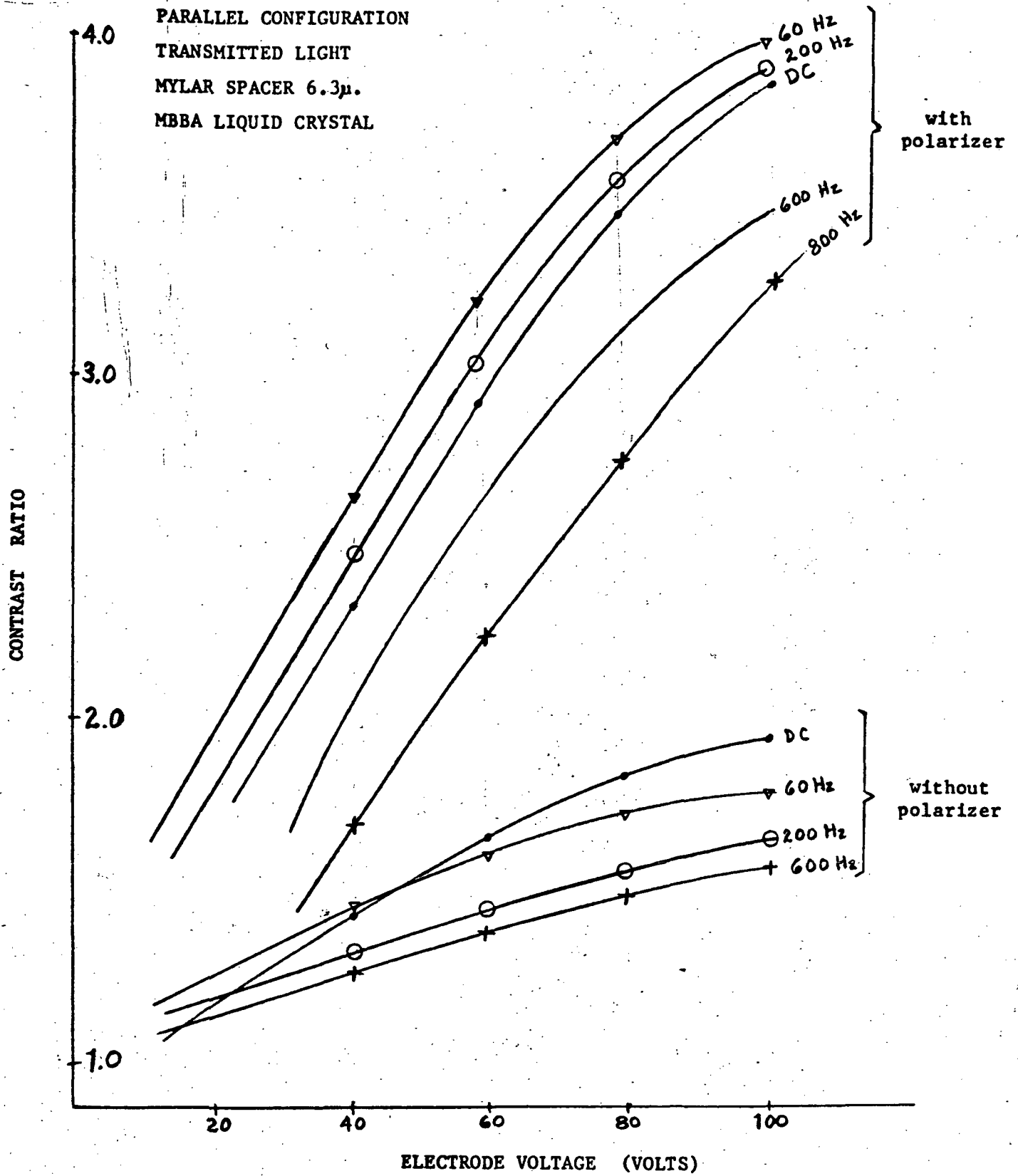
Figure 4.2

Contrast Ratio as a Function of Voltage   (Transmitted Light)

PARALLEL CONFIGURATION
TRANSMITTED LIGHT
MYLAR SPACER 12.7μ
MBBA LIQUID CRYSTAL

with polarizer

DC
60 Hz
400 Hz
800 Hz
1K Hz

without polarizer

DC
60 Hz
200 Hz
400 Hz
800 Hz

CONTRAST RATIO

ELECTRODE VOLTAGE   (VOLTS)
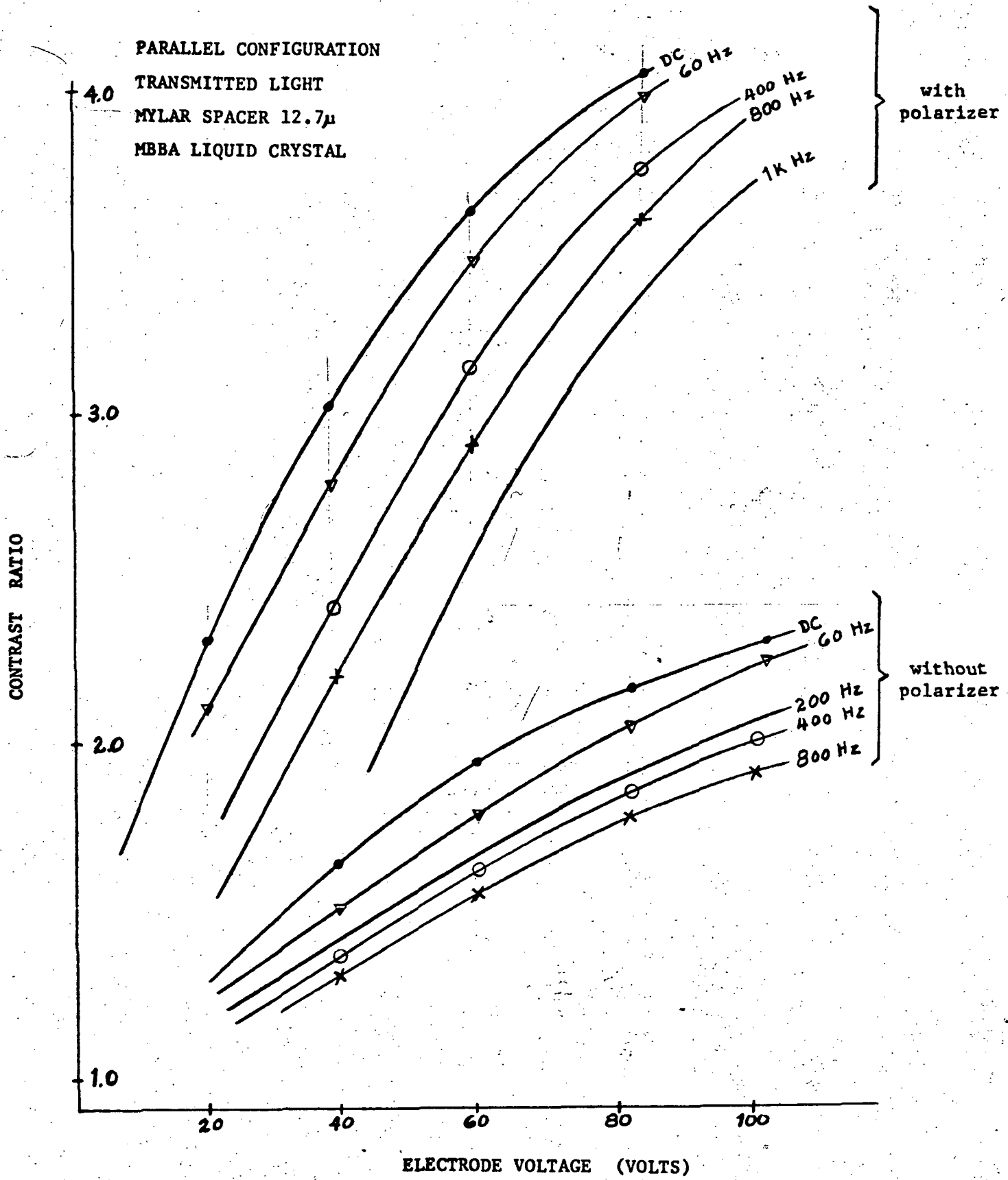
Figure 4.3

CONTRAST RATIO AS A FUNCTION OF VOLTAGE   (TRANSMITTED LIGHT)

PARALLEL CONFIGURATION
TRANSMITTED LIGHT
MYLAR SPACER 30μ
MBBA LIQUID CRYSTAL
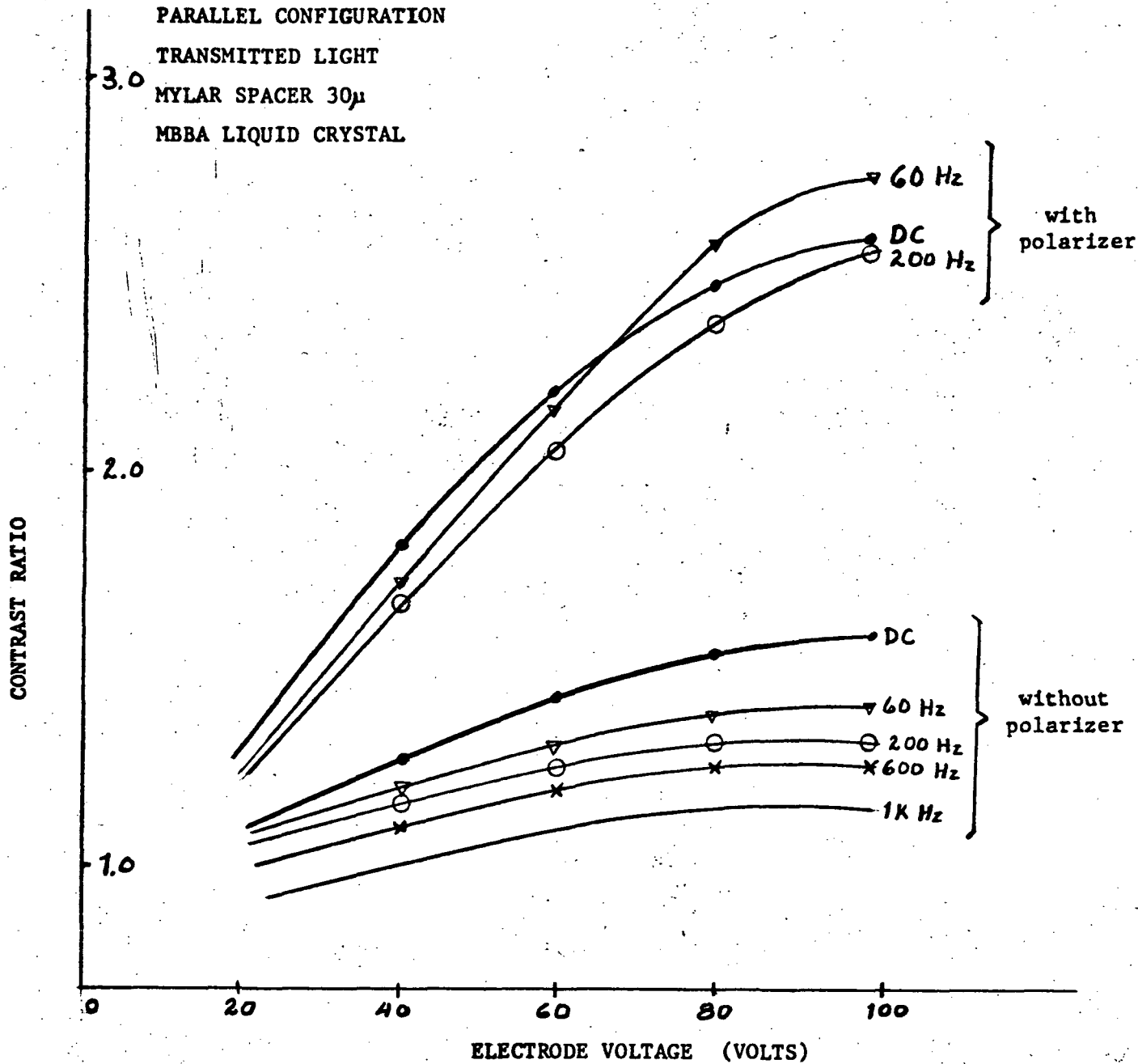
Figure 4.4

CONTRAST RATIO AS A FUNCTION OF VOLTAGE   (TRANSMITTED LIGHT)

CONTRAST RATIO AS A FUNCTION OF THICKNESS

PARALLEL CONFIGURATION
TRANSMITTED LIGHT
ELECTRODE VOLTAGE - 80 VOLTS
MBBA LIQUID CRYSTAL

WITH POLARIZER

WITHOUT POLARIZER

60 Hz

400 Hz

60 Hz

400 Hz

CONTRAST RATIO

THICKNESS (microns)

4.0

3.0

2.0

1.0

10

20

30
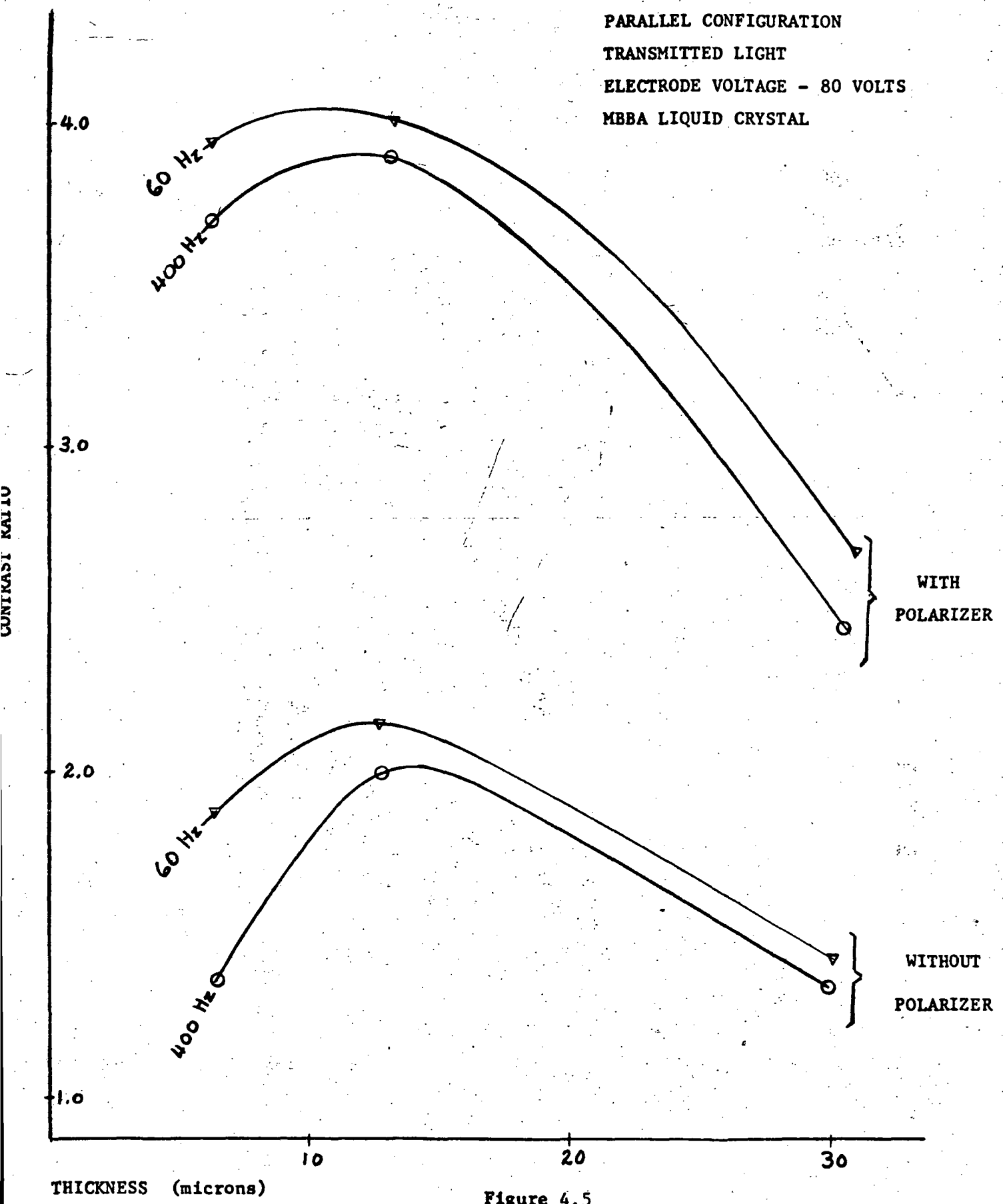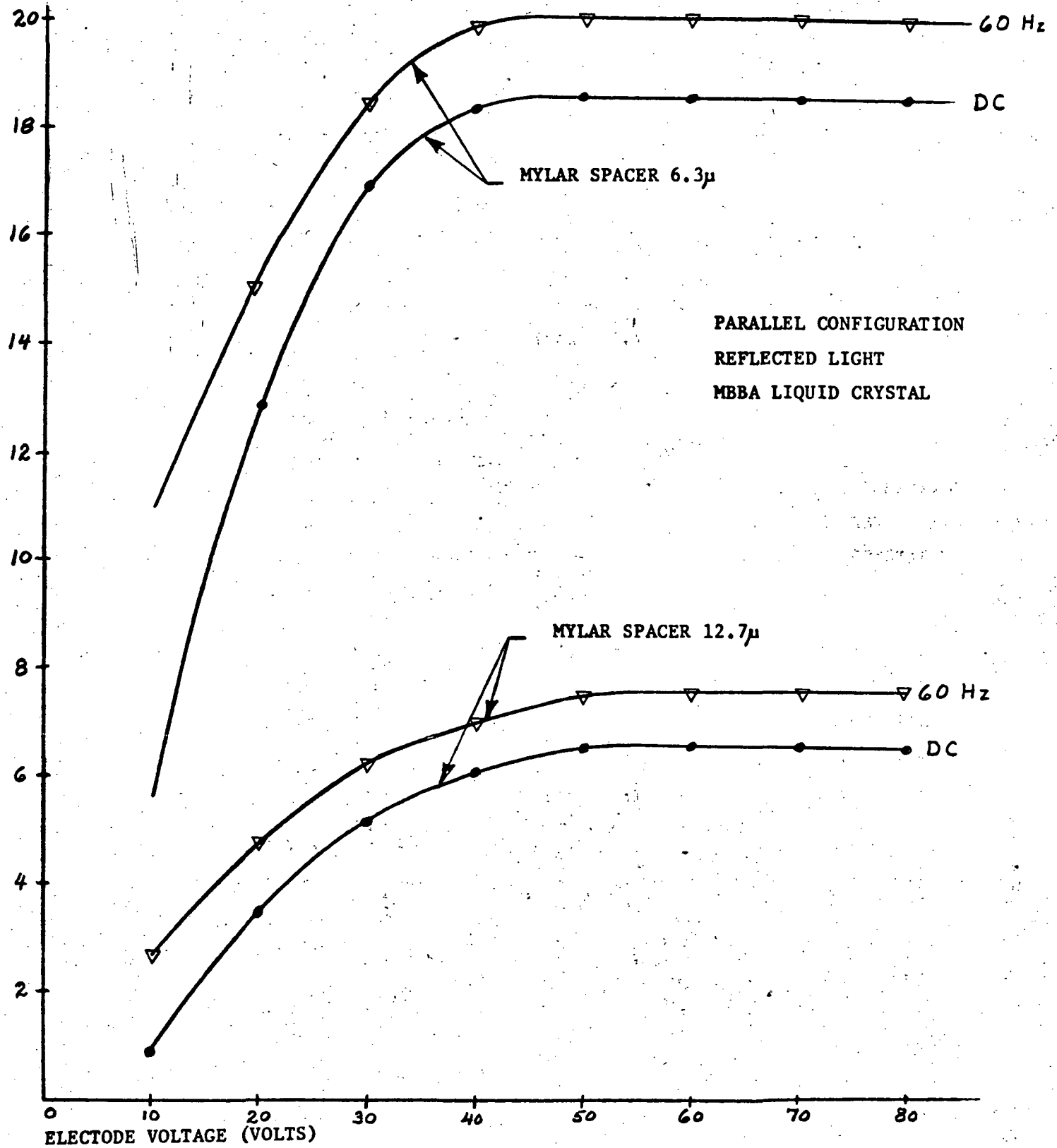
Figure 4.5

Figure 4.6
CONTRAST RATIO AS A FUNCTION OF VOLTAGE   (REFLECTED LIGHT)

PARALLEL CONFIGURATION
REFLECTED LIGHT
MBBA LIQUID CRYSTAL
MYLAR SPACER 30μ
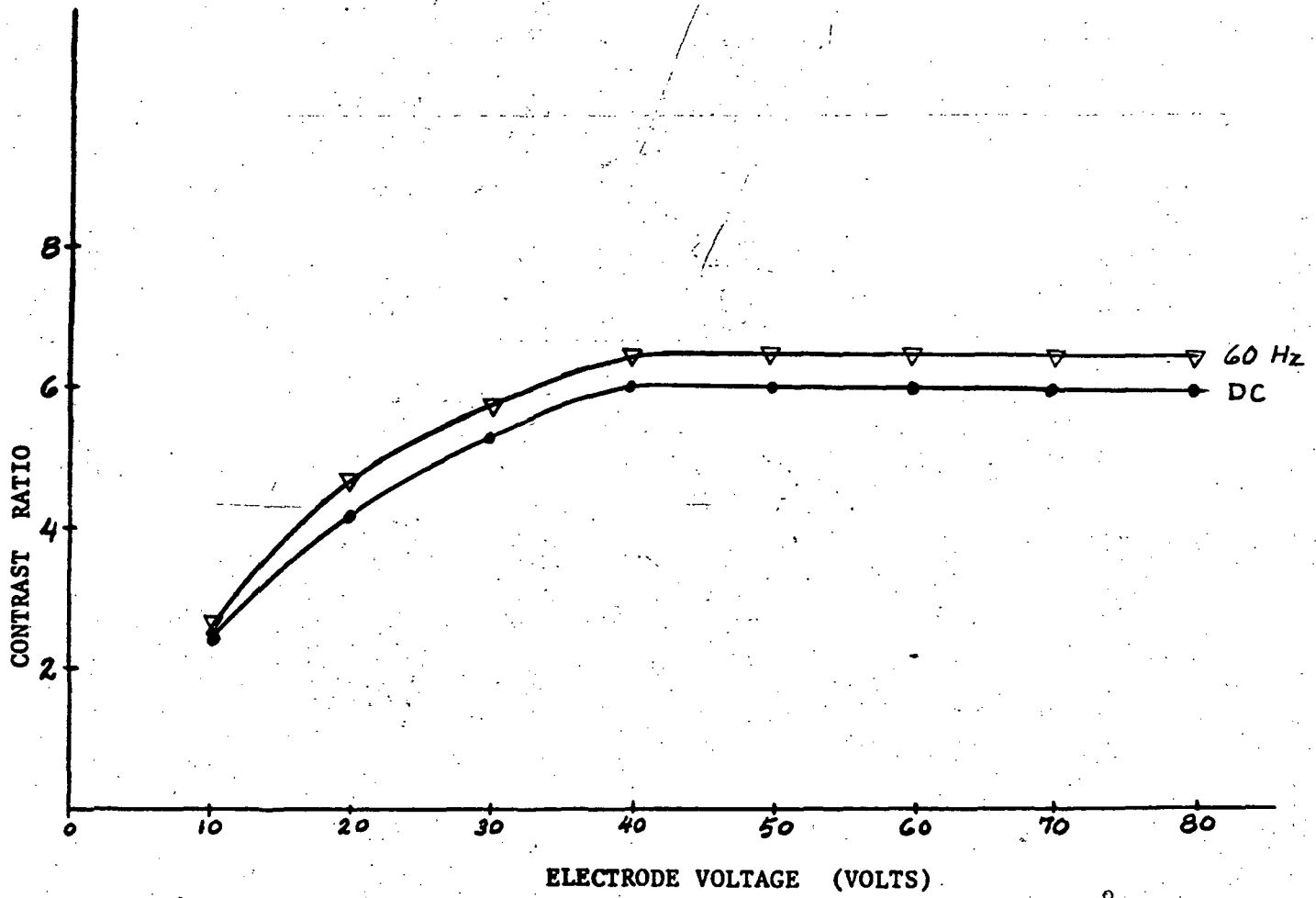
Figure 4.7

CONTRAST RATIO AS A FUNCTION OF VOLTAGE

PARALLEL CONFIGURATION
REFLECTED LIGHT
MBBA LIQUID CRYSTAL
ELECTRODE VOLTAGE – 70 VOLTS

THICKNESS (MICRONS)
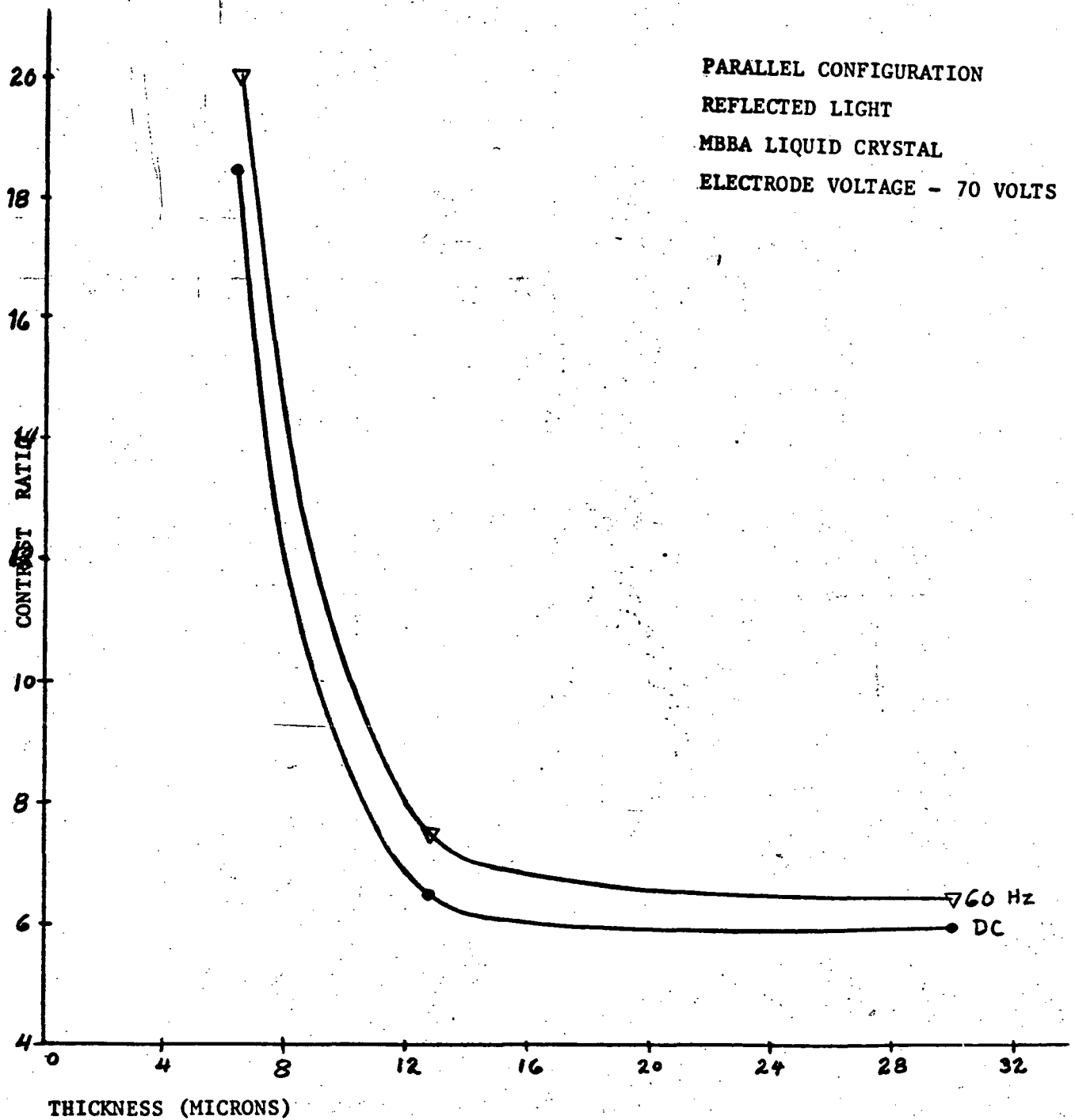
Figure 4.8

Contrast Ratio as a Function of Thickness (Reflected Light)
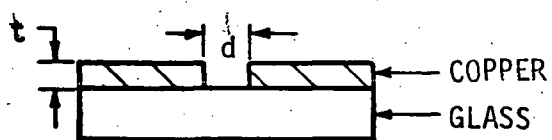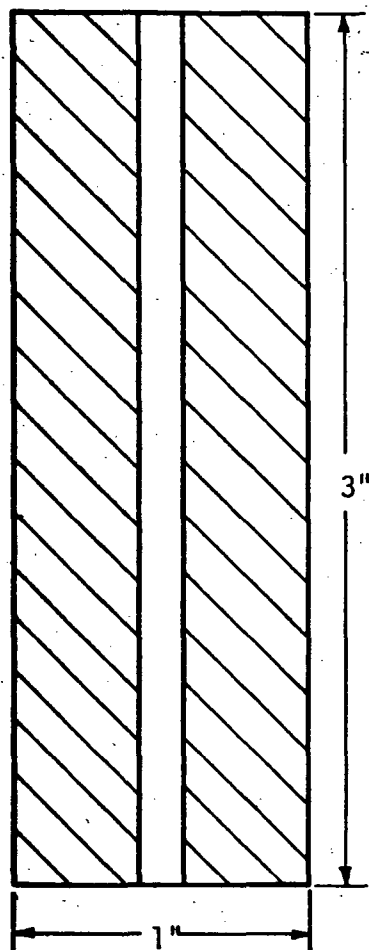
Figure 4.9

PERPENDICULAR CONFIGURATION TEST CELL
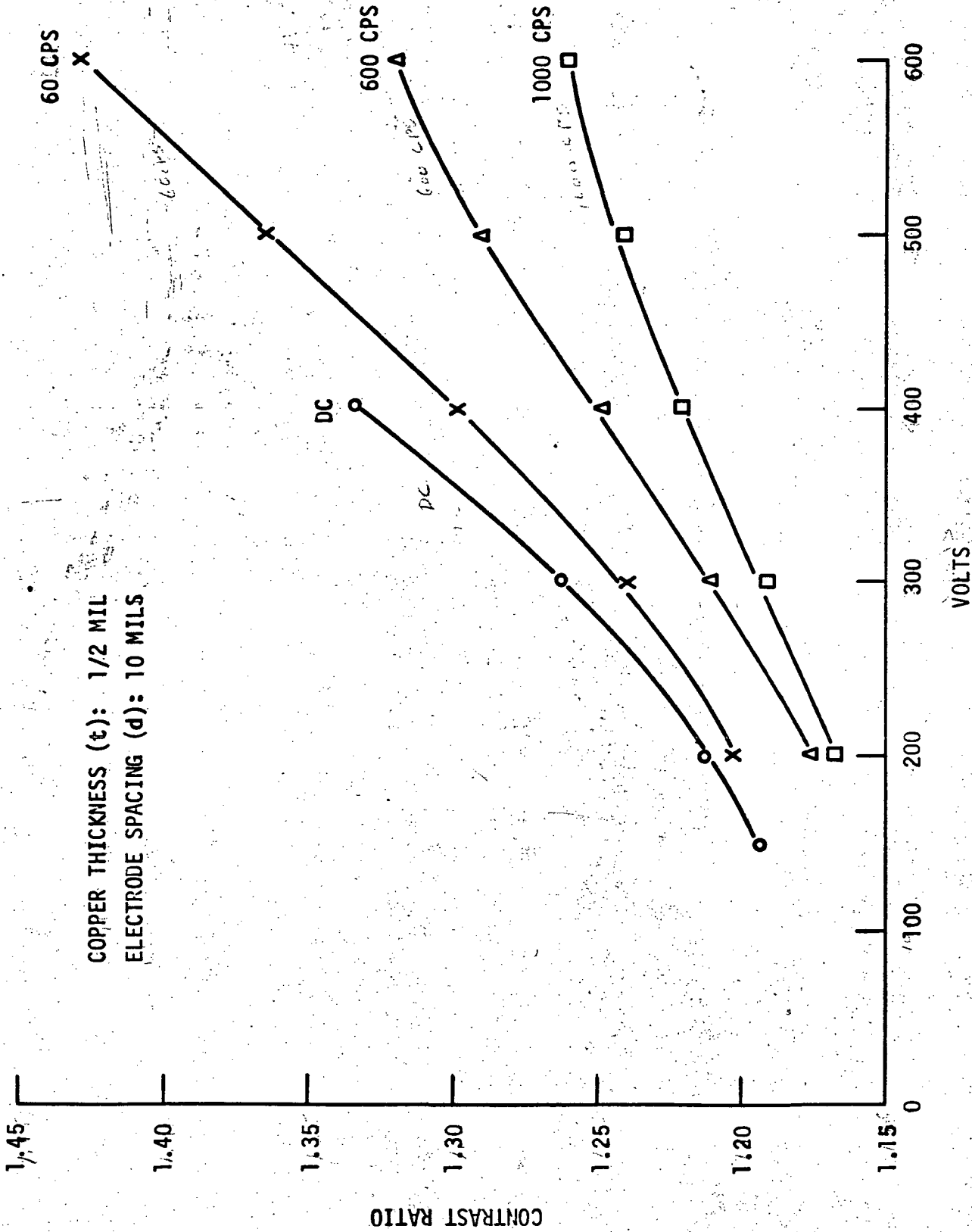
Figure 4.10

CONTRAST RATIO AS A FUNCTION OF VOLTAGE
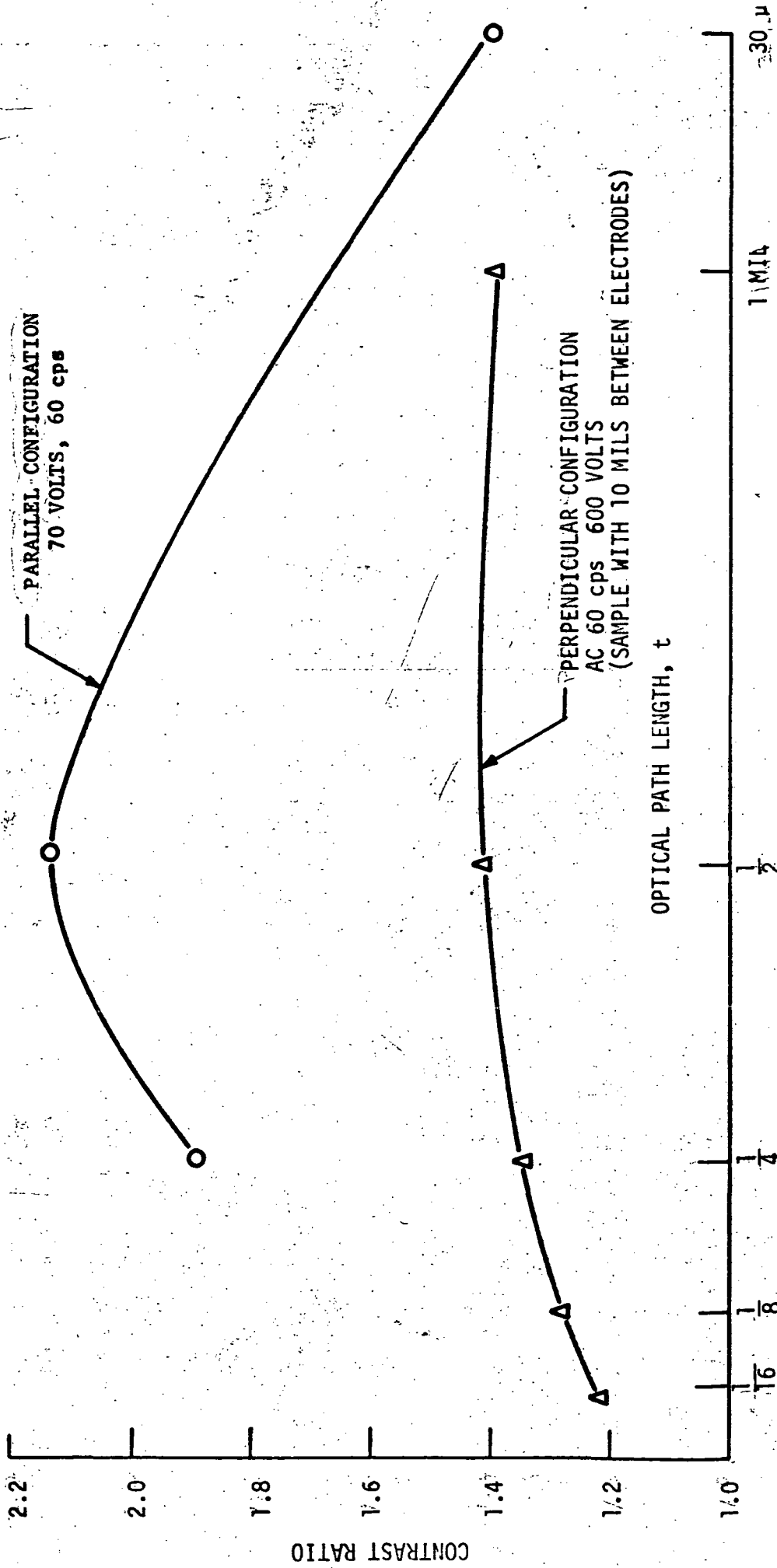
Figure 4.11

CONTRAST RATIO AS A FUNCTION OF OPTICAL PATH LENGTH
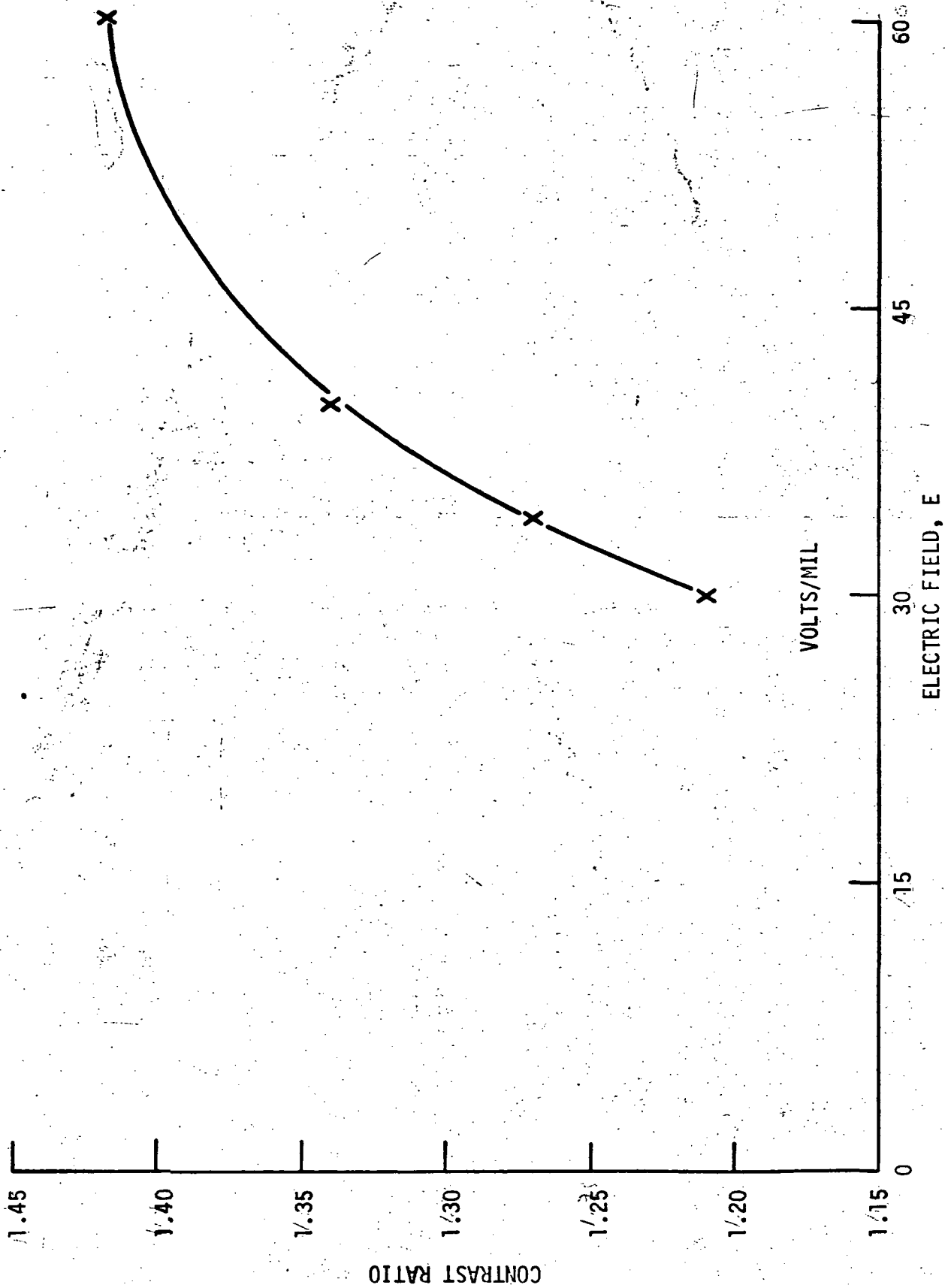
CONTRAST RATIO AS A FUNCTION OF ELECTRIC FIELD

Figure 4.12

ELECTRIC FIELD, E
VOLTS/MIL
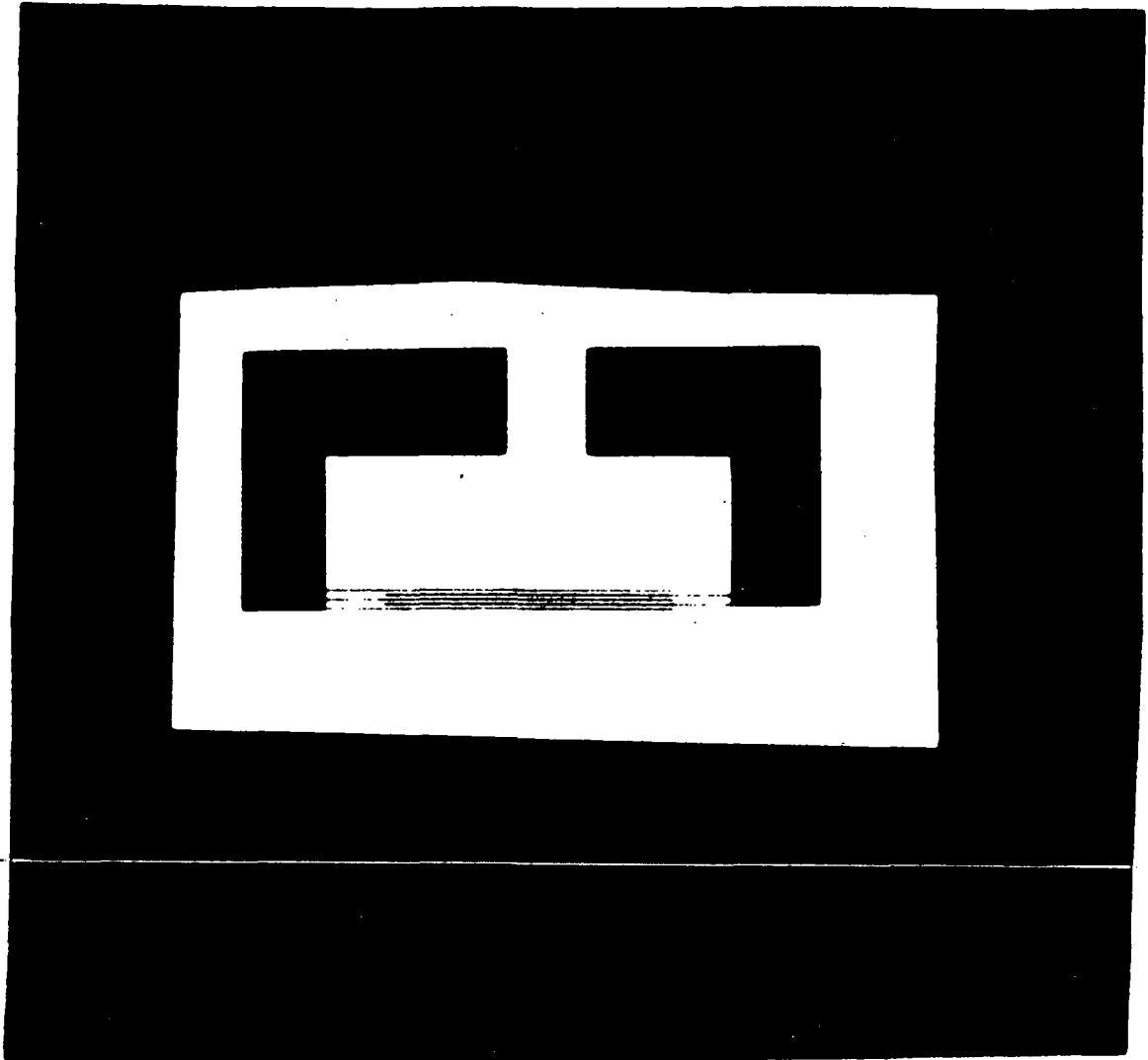
CONTRAST RATIO

Figure 4.13

MULTIPLE LINE GEOMETRY MASK
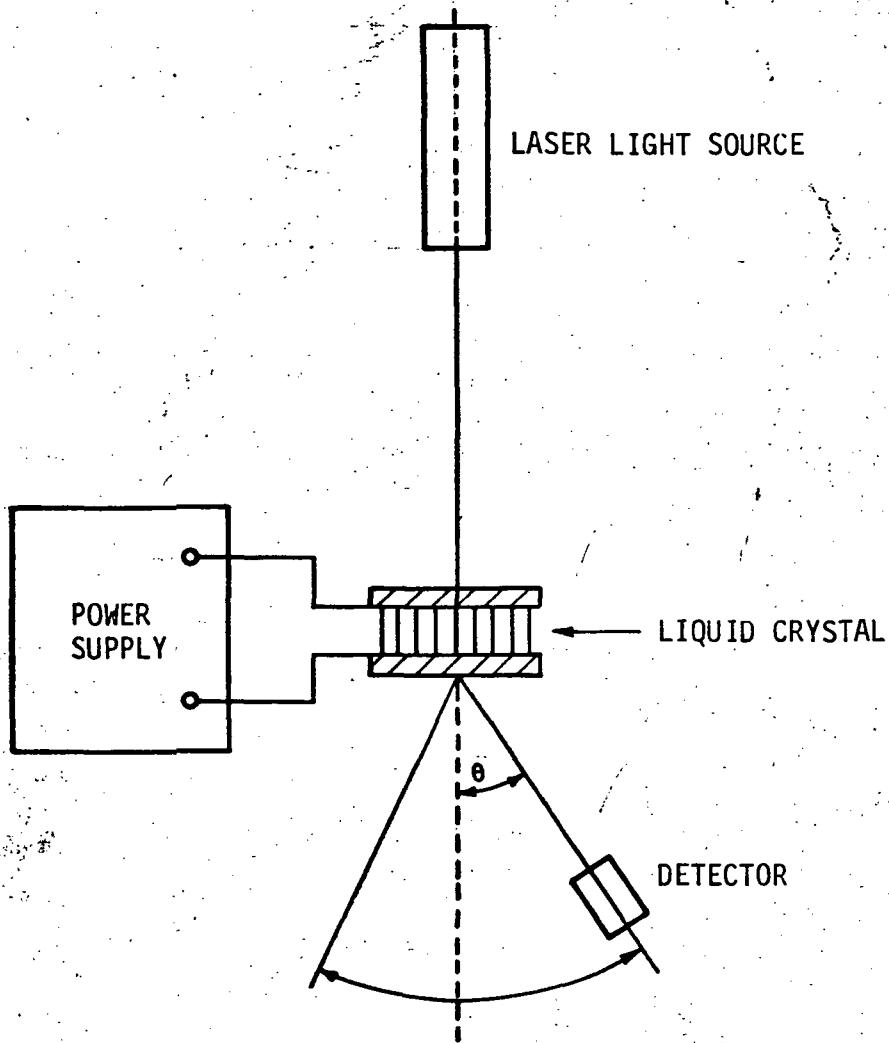
Figure 4.14

APPARATUS FOR MEASURING OFF AXIS CONTRAST RATIO

PARALLEL CONFIGURATION CELL
TRANSMITTED LIGHT
EXCITATION: 60 CPS

0 VOLTS

40 VOLTS

60 VOLTS

ANGLE (θ) (DEGREES)
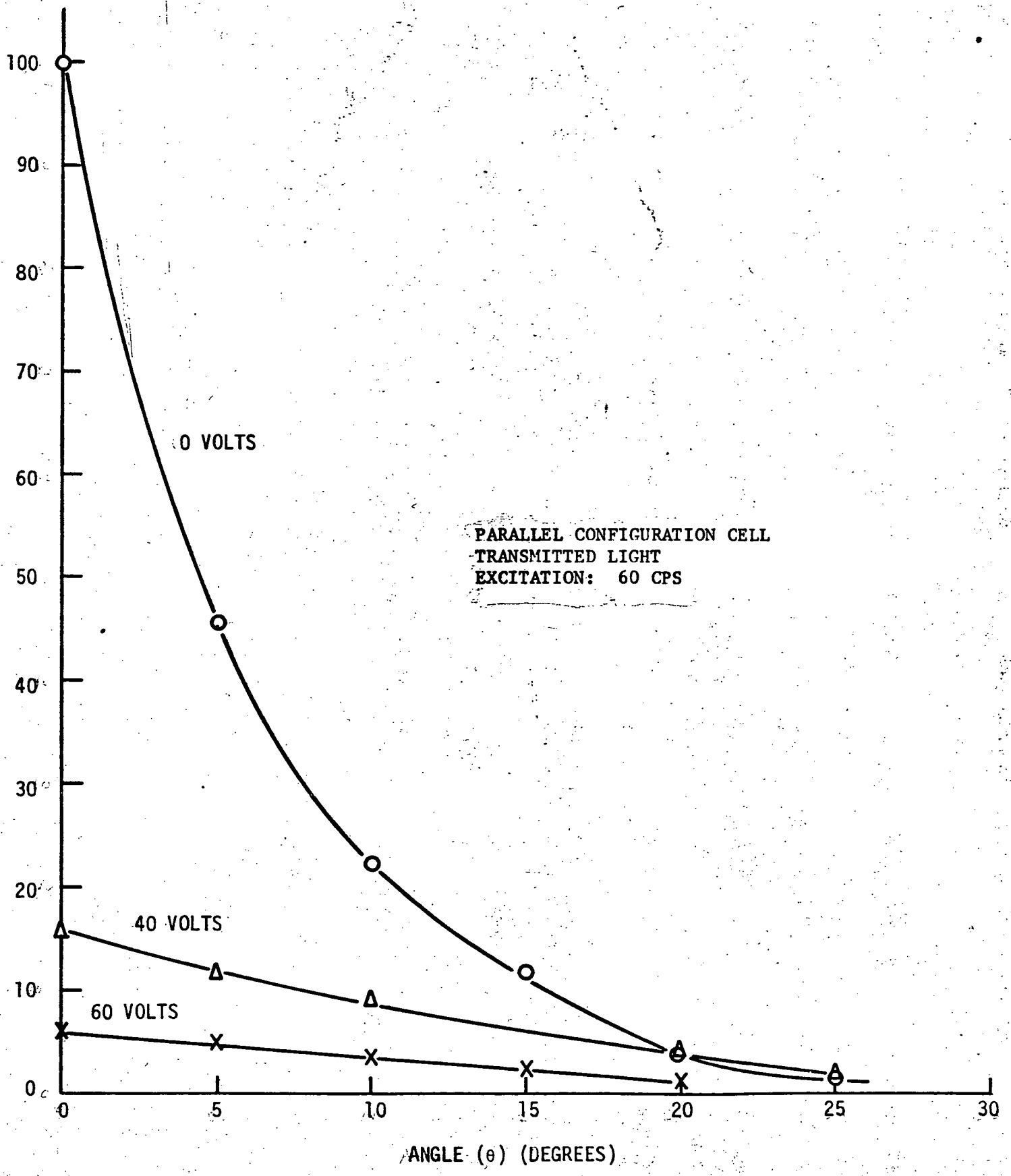
Figure 4.15
TRANSMISSION AS FUNCTION OF VIEWING ANGLE

LINE WIDTH IN MILS
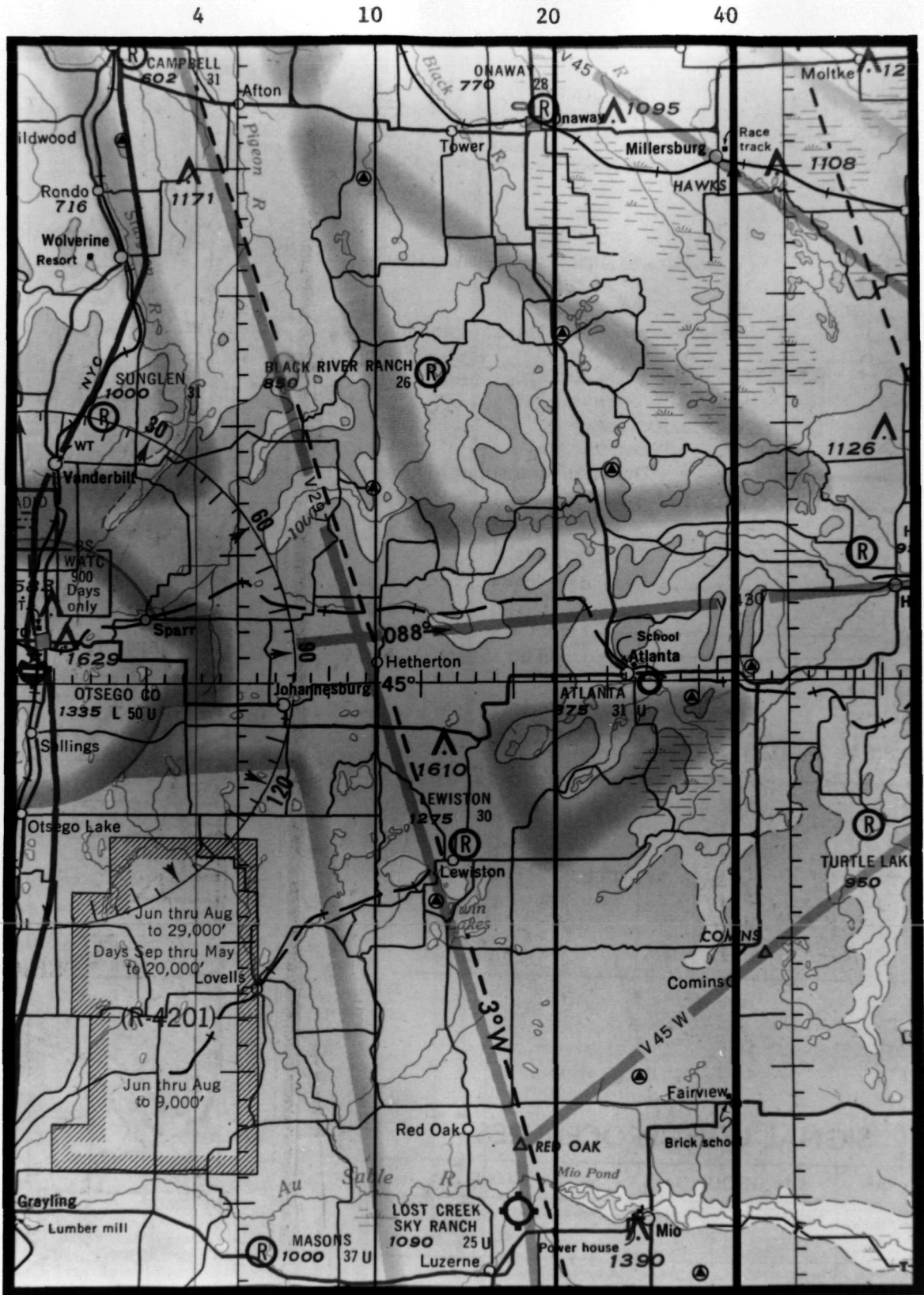
Figure 4.16

LEGIBILITY OF MAP WITH REFLECTIVE LINE OVERLAY
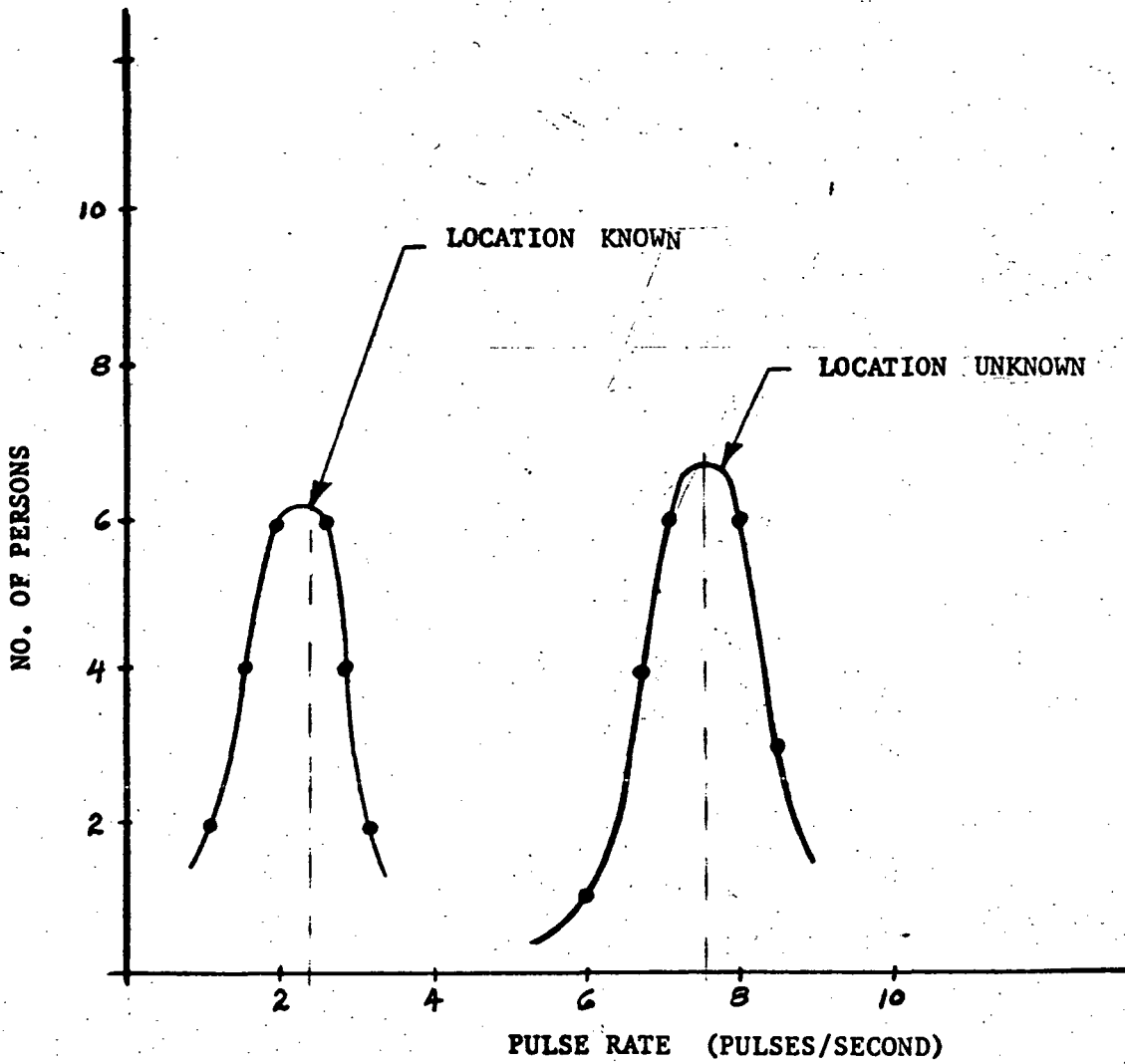
Figure 4.17

OPTIMUM REPETITION RATE

MBBA LIQUID CRYSTAL
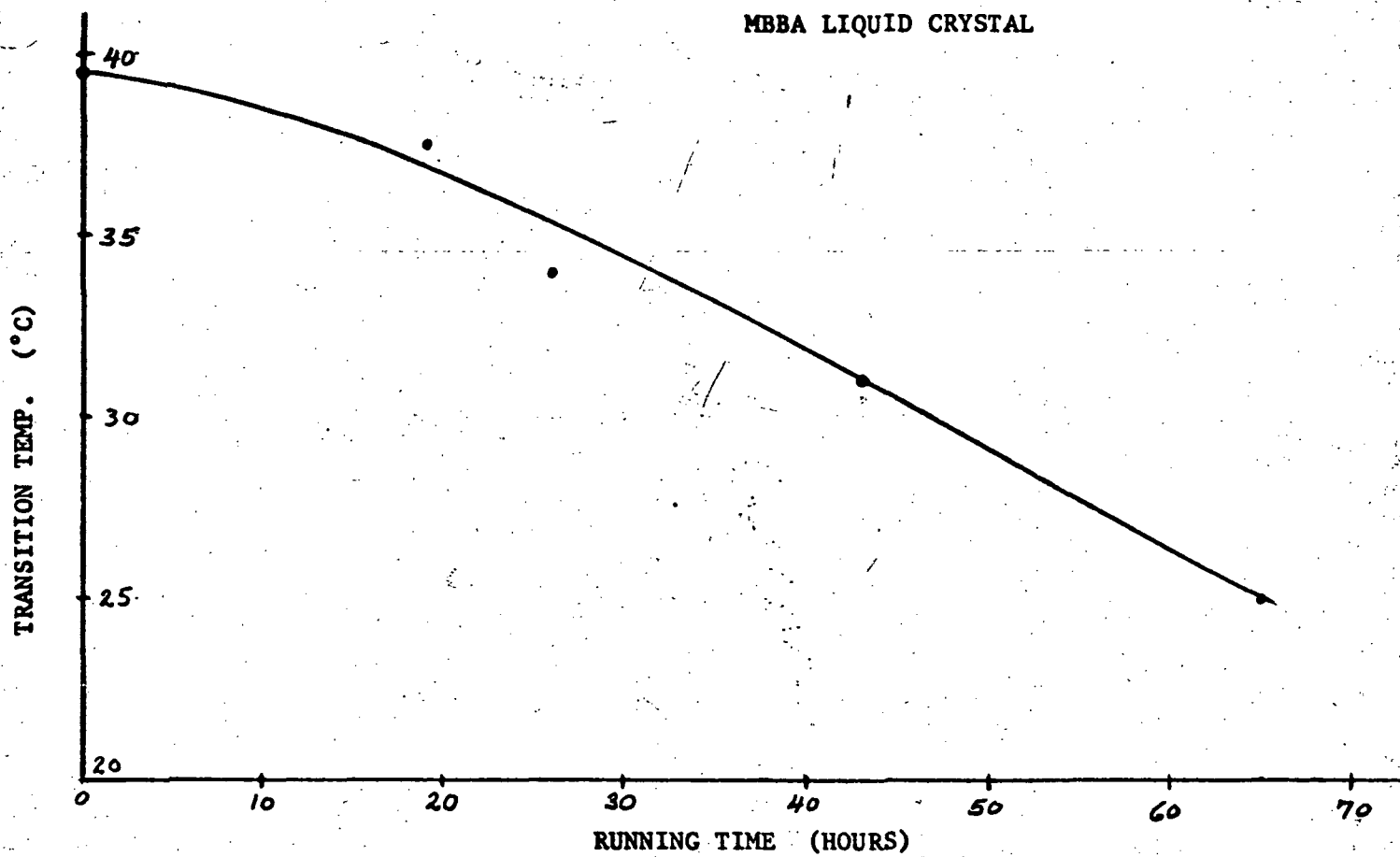
Figure 5.1

TRANSITION TEMPERATURE AS A FUNCTION OF AGING
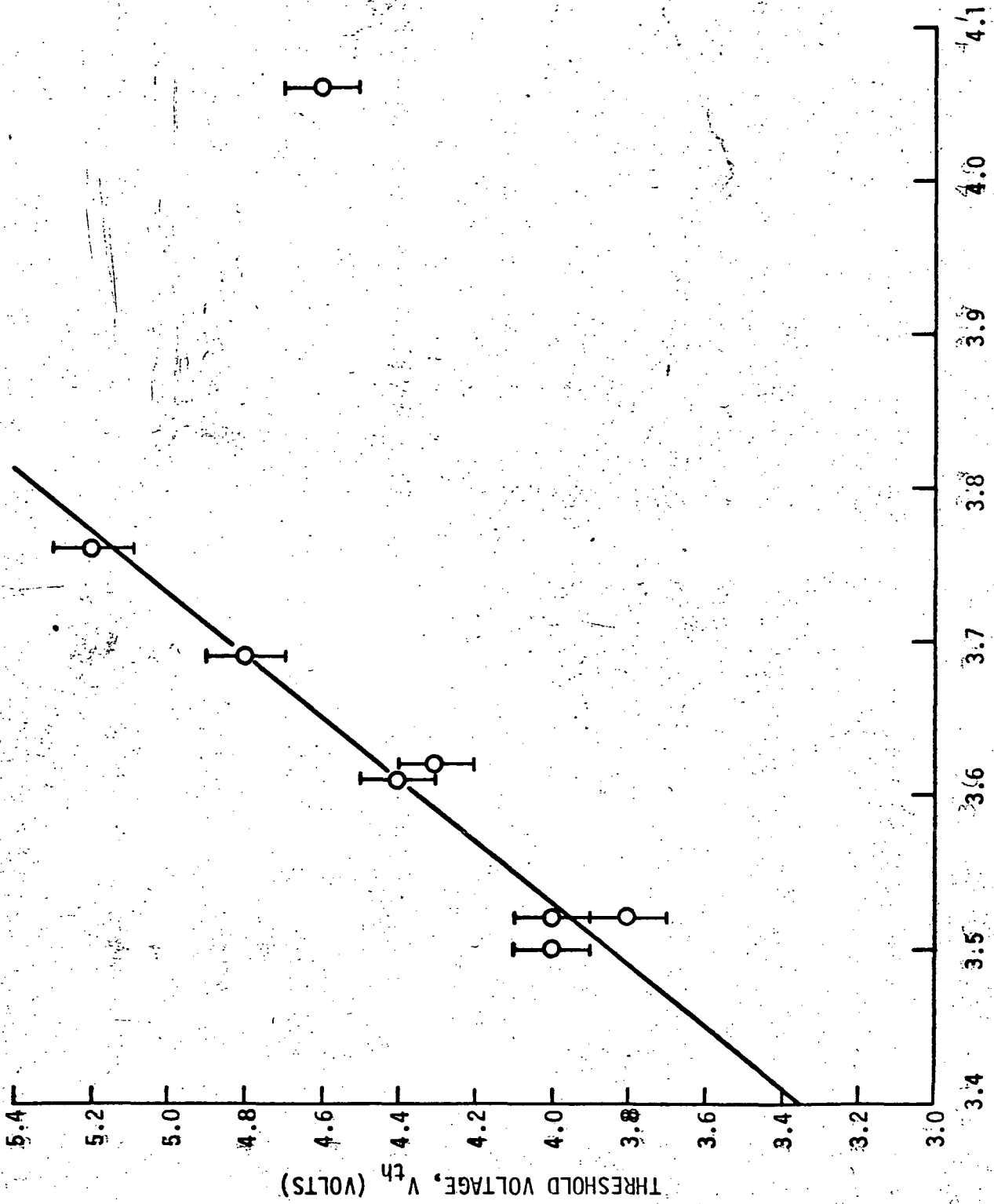
Figure 6.1

THRESHOLD VOLTAGE AS A FUNCTION OF DIELECTRIC CONSTANT

LIQUID CRYSTAL

LASER
BEAM

β γ

α

B FIELD NORMAL, MOLECULES
LINED UP NORMAL TO PAGE
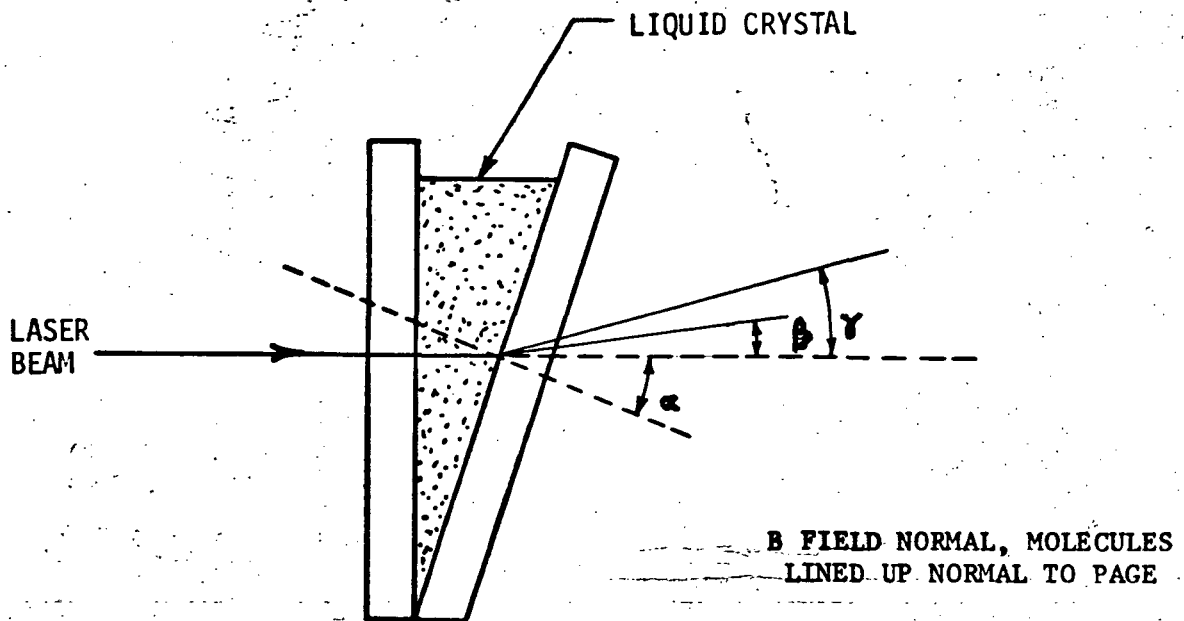
MOLECULES LINED UP NORMAL TO INCOMING BEAM WITH MAGNETIC FIELD

$$\Delta n = n_e - n_0 = \frac{\sin(\alpha+\gamma) - \sin(\alpha+\beta)}{\sin\alpha}$$

Figure 6.2
DETERMINATION OF BIREFRINGENCE
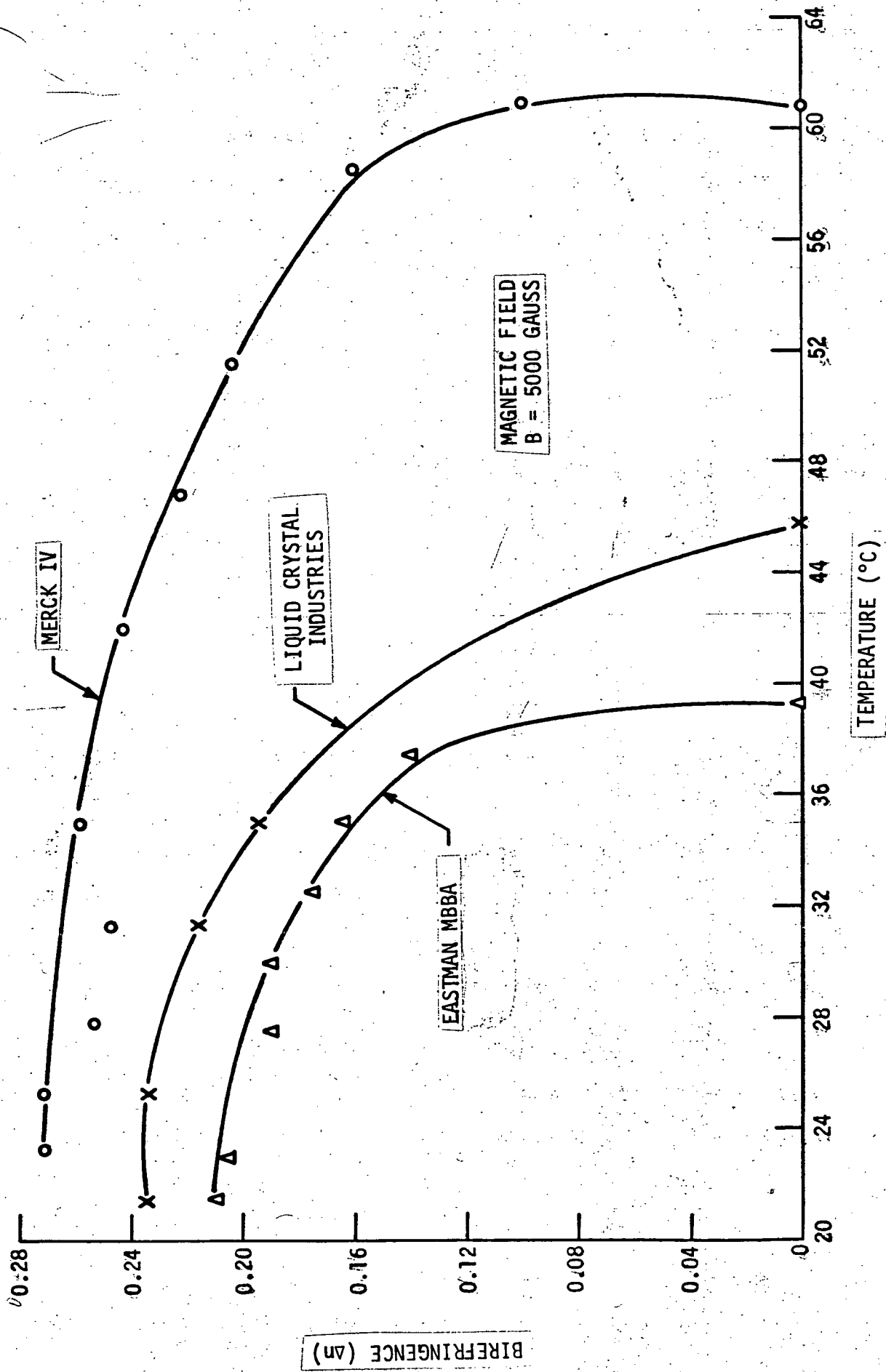
Figure 6.3

BIREFRINGENCE AS A FUNCTION OF TEMPERATURE

LINE DIMENSIONS IN MILS

4-40-4

4-20-4

4-10-4

4-5-4

Figure 7.1

PARALLEL LINE VISIBILITY
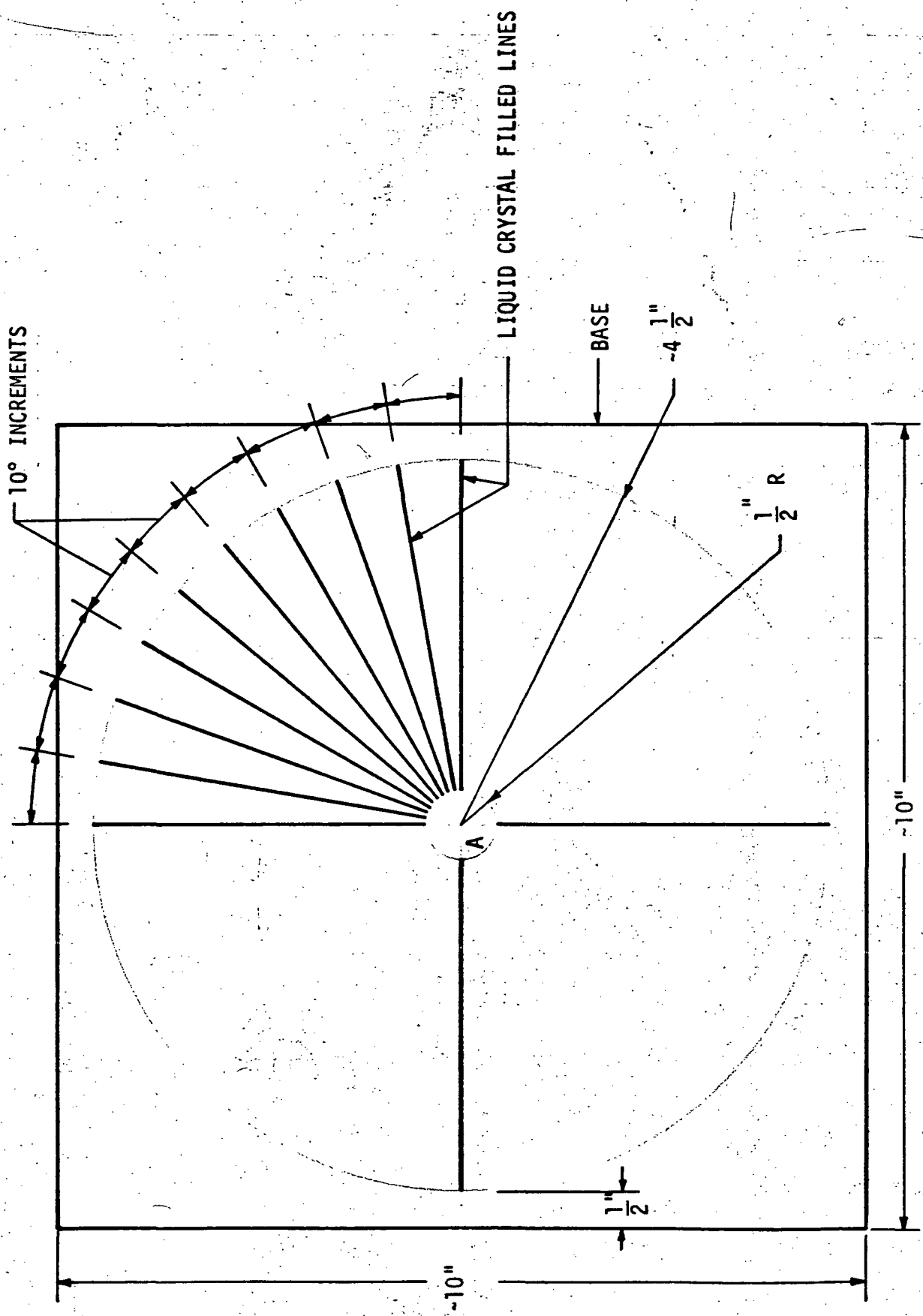
Figure 8.1

GENERAL CONFIGURATION OF DISPLAY MODEL

FIG. 8.1
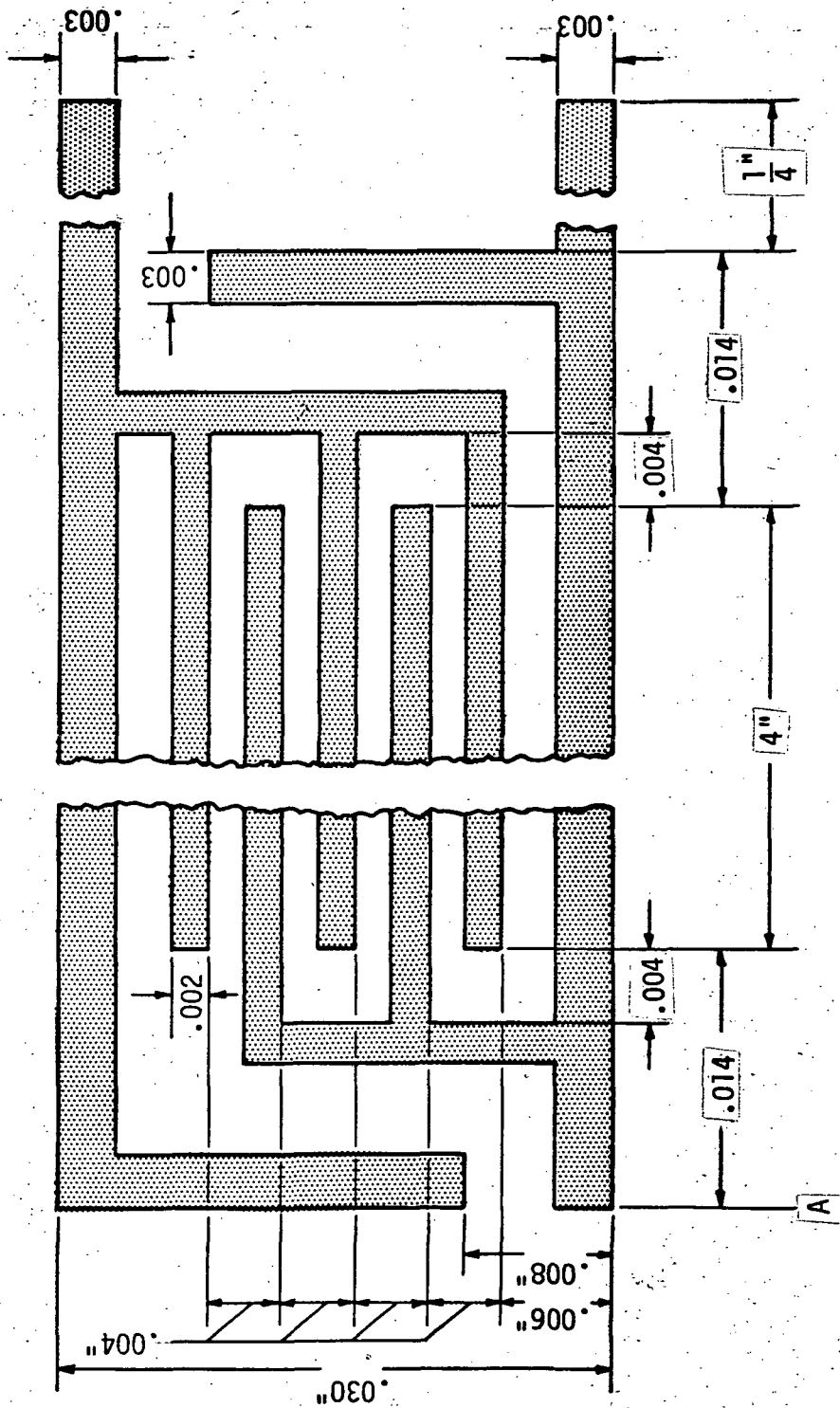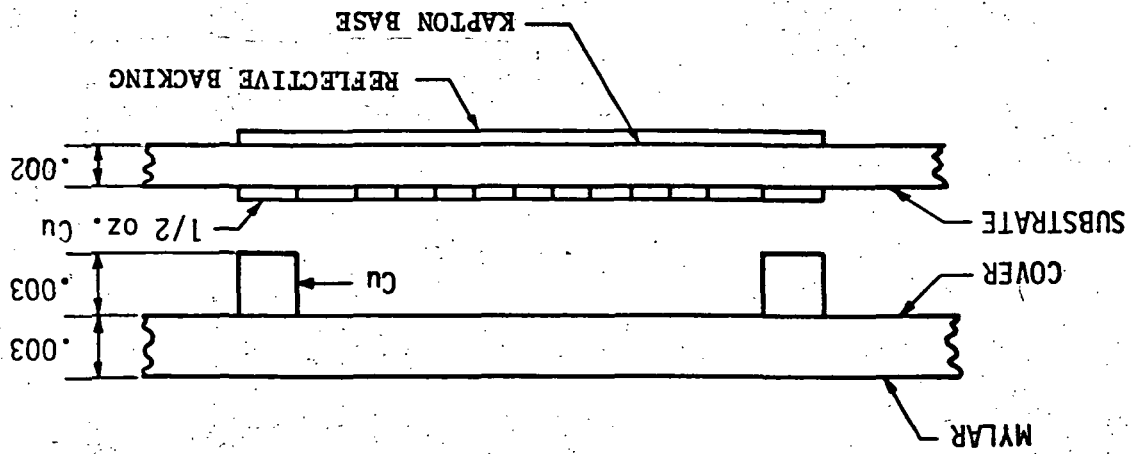
Figure 8.2

PERPENDICULAR CONFIGURATION LINE DETAIL
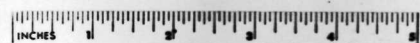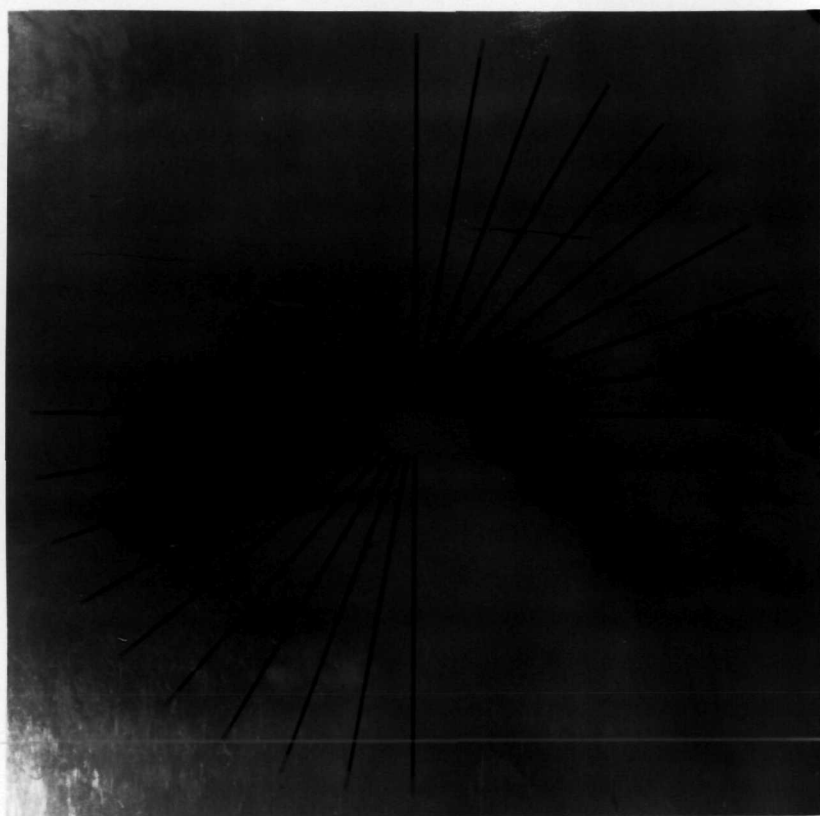
Figure 8.3

PHOTOGRAPH OF DISPLAY DEVICE
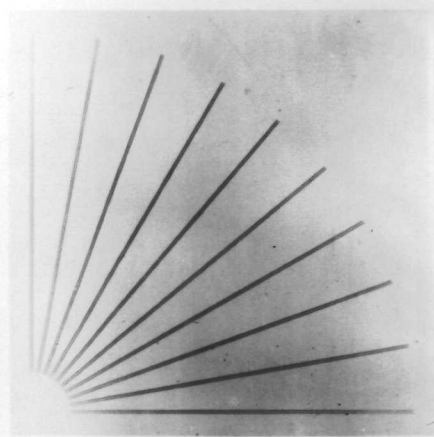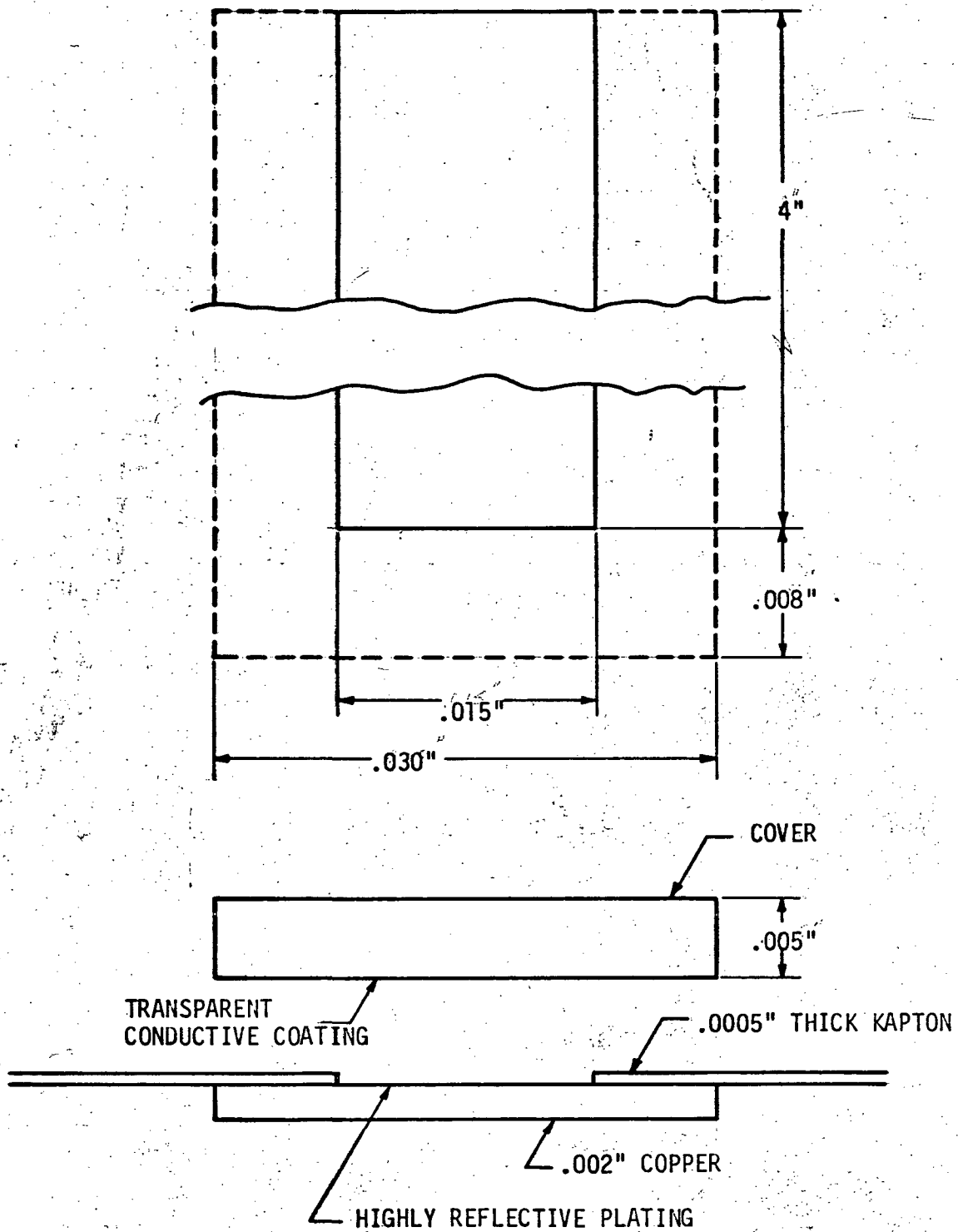
4"

.008"

.015"

.030"

COVER

.005"

TRANSPARENT
CONDUCTIVE COATING

.0005" THICK KAPTON

.002" COPPER

HIGHLY REFLECTIVE PLATING

Figure 8.4
PARALLEL CONFIGURATION LINE DETAIL